NJC

PAPER

View Article Online
View Journal

Cite this: DOI: 10.1039/c9nj01113g

Annulated bacteriochlorins for near-infrared photophysical studies†

Hikaru Fujita, [a] Haoyu Jing, [a] Michael Krayer, [a] Srinivasarao Allu, [a] Gorre Veeraraghavaiah, [a] Zhiyuan Wu, [a] Jianbing Jiang, [a] James R. Diers, [b] Nikki Cecil M. Magdaong, [c] Amit K. Mandal, [c] Arpita Roy, [c] Dariusz M. Niedzwiedzki, [d] Christine Kirmaier, [c] David F. Bocian, *[b] Dewey Holten *[c] and Jonathan S. Lindsey *[a]

Received 2nd March 2019,
Accepted 5th April 2019

DOI: 10.1039/c9nj01113g

rsc.li/njc

Molecules with strong absorption in the near-infrared (NIR) spectral region are of interest for a variety of applications in the photosciences. Nature's NIR absorbers are bacteriochlorophylls, which contain a tetrahydroporphyrin chromophore accentuated by attached auxochromes, including a β,*meso*-bridging isocyclic ring. Modification of the isocyclic ring has provided a convenient means of wavelength tuning. In other tetrapyrroles, annulation at the β,*meso*-, β,β-, and β-*meso*-β-positions also has enabled wavelength tuning. Here, synthetic bacteriochlorins bearing a *gem*-dimethyl group in each pyrroline ring have provided the foundation for studies of annulation. Seven new free base bacteriochlorins have been prepared and seven others have been elaborated therefrom. Six distinct routes known among porphyrins were explored. Ultimately, annulation of phenaleno or benzo groups at the β,*meso*-sites (*i.e.*, spanning the 3,5- and 13,15-positions) of bacteriochlorins was achieved by a new route that entails two successive Pd-mediated coupling reactions of a dibromobacteriochlorin with a bromoarylboronic acid. The corresponding **Phen-BC** or **Benz-BC** absorbs at 913 or 1033 nm, respectively. Examination by time-resolved spectroscopy revealed an excited-state lifetime of 150 ps or 7 ps, with commensurably low fluorescence quantum yield (Φ_f) values estimated to be ~0.004 or 3×10^{-5}, respectively. The origin of the short excited-state lifetimes due to β,*meso*-annulation is unknown, but is not simply a consequence of the energy-gap law for non-radiative decay.

Introduction

Bacteriochlorins are attractive candidates for diverse photophysical studies such as artificial photosynthesis, photodynamic therapy, and optical imaging owing to their strong absorption in the near-infrared (NIR) region.[1] Bacteriochlorophyll *a*, the core light absorber in anoxygenic photosynthetic bacteria, contains the bacteriochlorin chromophore along with an "isocyclic ring" spanning positions 13–15 (Chart 1).[2] The isocyclic ring is a 5-membered ring containing a keto group conjugated with the bacteriochlorin π-system at the 13-position, but a saturated methylene unit at the 15-position. Hence, the isocyclic ring (an annulated oxocyclopentano motif) does not cause conjugation to be extended across the 13,15-positions. The full complement of substituents about the perimeter of the macrocycle has precluded studies to install annulated rings to the native bacteriochlorophylls; however, the allomerization of the isocyclic ring has been exploited to create bacteriochlorin-imides (often referred to as bacteriopurpurinimides).[3,4]

In previous studies, a synthetic bacteriochlorin was annulated with imide rings in an effort to extend the position of the long-wavelength absorption (Q_y) band deeper into the NIR spectral region. For the bacteriochlorin constructed with imides annulated at the 2,3- and 12,13-positions (*i.e.*, β,β-annulation), the Q_y band appeared at 800 nm.[5] On the other hand, the bacteriochlorin constructed with imides annulated at the 3,5- and 13,15-positions (*i.e.*, β,*meso*-annulation) gave the Q_y band at 875 nm.[5]

[a] Department of Chemistry, North Carolina State University, Raleigh, North Carolina 27695-8204, USA. E-mail: jlindsey@ncsu.edu; Tel: +1-919-515-6406
[b] Department of Chemistry, University of California, Riverside, California 92521-0403, USA. E-mail: david.bocian@ucr.edu; Tel: +1-951-827-3660
[c] Department of Chemistry, Washington University, St. Louis, Missouri, 63130-4889, USA. E-mail: holten@wustl.edu; Tel: +1-314-935-6502
[d] Department of Energy, Environmental & Chemical Engineering and Center for Solar Energy and Energy Storage, Washington University, St. Louis, Missouri 63130-4889, USA

† Electronic supplementary information (ESI) available: Extensive results concerning exploration of alternative routes; spectroscopic data for bacteriochlorin **BC-2**; ^{1}H and ^{13}C NMR spectra for all new compounds on the route to **Phen-BC** and **Benz-BC**; and single-crystal X-ray data. CCDC 1900109 (**21**), 1900117 (**24**) and 1900118 (**18**). For ESI and crystallographic data in CIF or other electronic format see DOI: 10.1039/c9nj01113g

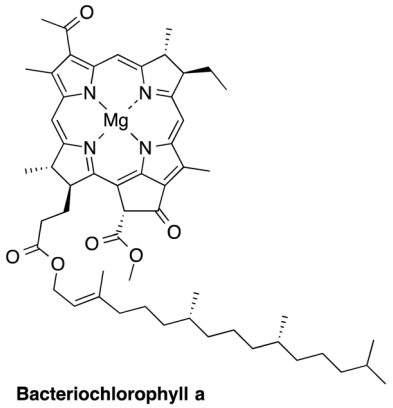

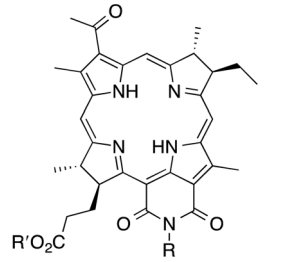

Chart 1 Structure of bacteriochlorophyll *a* and bacteriopurpurinimides.

One distinction between the two types of bis(imide)s is that β,β-annulation affords a 5-membered ring whereas β,*meso*-annulation gives a 6-membered ring. The bacteriochlorin-β,β-bis(imide) **MeO-I2-ββ-BC** gave a singlet excited-state lifetime (τ_s) of 3.6 ns and fluorescence quantum yield (Φ_f) value of 0.17 in toluene.[5] In contrast, the bacteriochlorin-β,*meso*-bis(imide) **I2-BC** gave τ_s = 1.0 ns and Φ_f = 0.027 in the same solvent.[5] A synthetic bacteriochlorin bearing a single β,*meso*-imide (**I-BC**) was prepared and found to exhibit Q_y = 818 nm, τ_s = 1.9 ns and Φ_f = 0.036 in toluene.[6] The shorter lifetime and diminished fluorescence quantum yield with the β,*meso*-imides were surprising and of unknown origin.

The annulation of tetrapyrroles with aromatic rings has long been pursued as a means to impart a bathochromic shift to the long-wavelength absorption band.[7–12] Issues concerning annulated tetrapyrroles are ease of synthetic access, solubility, stability, photophysical characterization, and absorption and fluorescence in the deep NIR region. Annulation with aromatic rings at the *meso*-positions is a common strategy to synthesize β,*meso*- (and also β,*meso*,β-) annulated porphyrins. Popular methods for annulation with aromatic hydrocarbons include oxidative coupling[13–26] and palladium-catalyzed intramolecular direct arylation.[27–31] On the other hand, β,β-annulated porphyrins have chiefly been prepared by (1) porphyrin formation from a β,β-annulated pyrrole, or (2) aromatization of a peripheral non-aromatic ring, which often involves prior cyclization of β substituents.[7–9,12] Synthesis of the β,β-annulated porphyrins has been chiefly pioneered by Lash[7,8] whereas β,*meso*-annulations with porphyrins have been deeply investigated by a number of groups.[32,33] These strategies developed with porphyrins in principle can be applied to the synthesis of β,*meso*- or β,β-annulated bacteriochlorins, albeit with two caveats: (1) in practice, the synthetic chemistry of bacteriochlorins has significantly lagged that of porphyrins; and (2) the reactivity of bacteriochlorins appears to be somewhat different from that of porphyrins.

Representative synthetic approaches to bacteriochlorins[1,34] include hydrogenation of porphyrins,[35,36] cycloaddition to porphyrins,[37] breaking and mending of porphyrins,[38] semisynthesis beginning typically with bacteriochlorophyll *a*,[3,4,39] and *de novo* synthesis. In *de novo* synthesis, the saturation characteristic of the pyrroline rings is built into the acyclic precursors to the bacteriochlorin macrocycles. Examples include the synthesis of tolyporphins[40,41] and a general route that we have been developing,[42–47] which has been extended imaginatively by others.[48–57]

In this paper, we report synthetic approaches for annulation of *de novo* synthesized bacteriochlorins. Installing annulated groups proved more challenging with bacteriochlorins than appears to be the case with porphyrins, as numerous established approaches with porphyrins such as oxidative coupling were unsuccessful. Ultimately, two β,*meso*-annulated bacteriochlorins were synthesized *via* palladium-catalyzed intramolecular arylation. Photophysical studies were performed to determine the lowest excited singlet-state lifetimes and fluorescence quantum yields. These studies were accompanied by density functional theory (DFT) calculations to examine the forms of the frontier molecular orbitals (MOs) and by time-dependent DFT (TDDFT) to compare the calculated *versus* observed absorption spectra.

Results

Synthetic approach toward β,β-annulated bacteriochlorins

We first focused on the synthesis of β,β-annulated bacteriochlorins. Thus, β,β-dibromodihydrodipyrrin-acetal **1**[54] was treated with $BF_3{\cdot}OEt_2$ in MeCN following the standard procedure for the self-condensation leading to synthetic bacteriochlorins[42] (Scheme 1). As a result, tetrabromobacteriochlorin **BC-1**, a potential precursor of β,β-annulated bacteriochlorins, was obtained in 16% yield. Bacteriochlorin **BC-1** differs from the tetrabromobacteriochlorin prepared by Oliveira and coworkers[54] in lacking a 5-methoxy group. The Mizoroki–Heck reaction of **BC-1** and methyl acrylate afforded tetrakis(methoxycarbonylvinyl)bacteriochlorin **BC-2** in 32% yield. However, oxidative cyclization of the adjacent methoxycarbonylvinyl groups leading to the corresponding β,β-annulated bacteriochlorin was unsuccessful, although the corresponding reaction of porphyrins affords β,β-benzoporphyrins.[58–67]

Next, phenanthropyrrole **2**[68] was selected as a starting material for the synthesis of β,β-phenanthrobacteriochlorin **BC-3**, similar to the synthesis of phenanthroporphyrins.[68,69] Following an established procedure,[44] phenanthropyrrole **2** was converted *via* the standard intermediates **3–6** to give dihydrodipyrrin-carboxaldehyde **7** in 5 steps (Scheme 2). The self-condensation of **7** in neat TFA, conditions used previously for β,β-substituted dihydrodipyrrin-carboxaldehydes,[44] gave bacteriochlorin **BC-3** as evidenced by laser-desorption mass

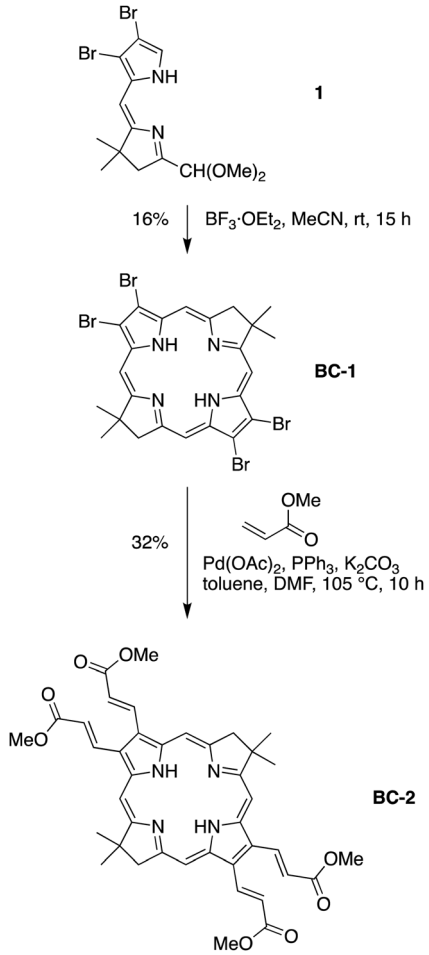

Scheme 1 Synthesis of tetrakis[(methoxycarbonyl)vinyl]bacteriochlorin **BC-2** *via* (tetrabromo)bacteriochlorin **BC-1**.

spectrometry (LD-MS, m/z = 671, $[M + H]^+$) and spectroscopic analysis (bacteriochlorin-like Q_y band absorption and fluorescence at 801 and 808 nm in CH_2Cl_2, respectively, Fig. 1) of a partially purified sample. However, quality NMR spectra could not be obtained due to the limited solubility of **BC-3** in organic solvents. Moreover, isolation of **BC-3** in pure form was thwarted by gradual decomposition. Adventitious oxidation in air may explain the instability of **BC-3** because a major contaminant, which increased gradually upon handling of **BC-3**, was attributed to the corresponding oxobacteriochlorin[5] given the characteristic data from LD-MS (m/z = 685, $[M + H]^+$) and absorption spectroscopy (Q_y band at 758 nm in CH_2Cl_2).

We envisaged that β,β-annulated bacteriochlorins might be stabilized by installation of electron-withdrawing groups, which by adding slight steric protrusions from the plane of the macrocycle might also provide improved solubility. However, attempts to install ester or imide moieties into the macrocycle were unsuccessful. The attempted syntheses are summarized in Chart S1 and Schemes S1–S10 (ESI†), and the synthesis and characterization data are provided for 15 new compounds (see the ESI†). The limitations of these routes prompted investigation of methods of oxidative annulation of appended aryl rings.

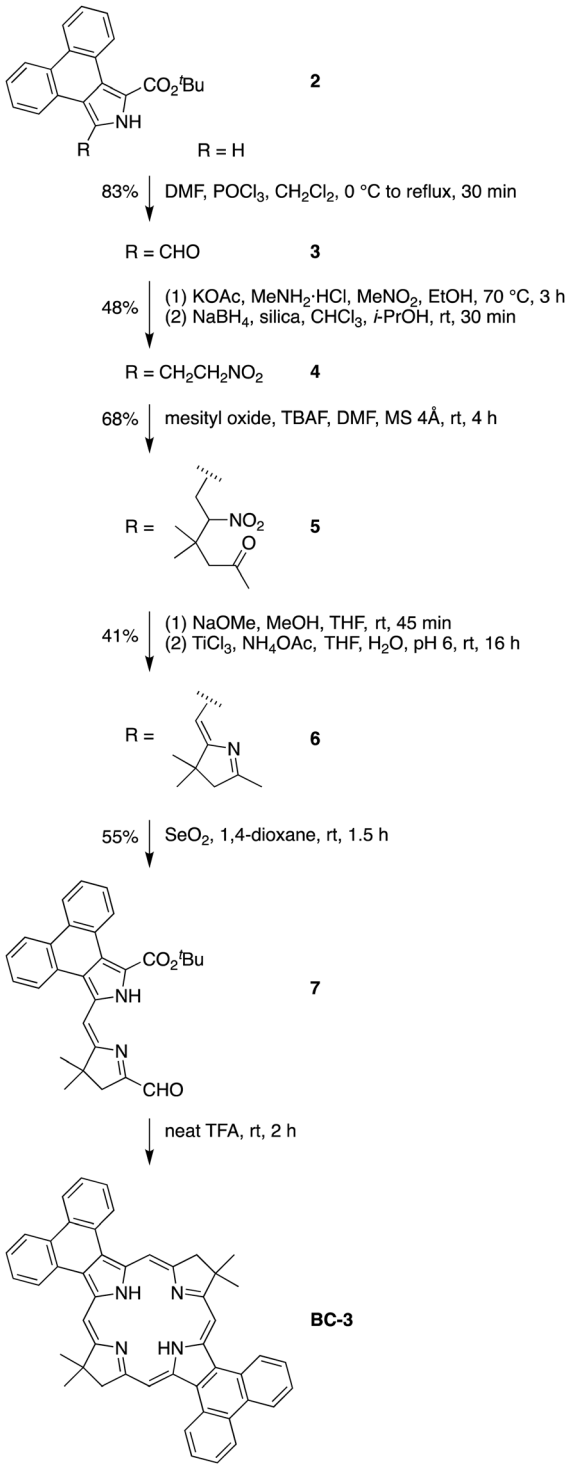

Scheme 2 Attempted synthesis of β,β-phenanthrene-annulated bacteriochlorin **BC-3**.

Synthetic approach toward β,*meso*-annulated bacteriochlorins *via* oxidative annulation

As the oxidative annulation of peripheral aromatic hydrocarbons is well-known for the synthesis of β,*meso*-annulated porphyrins, di(1-naphthyl)bacteriochlorins **BC-4–8** were prepared from **8**[70] (Scheme 3) for attempted transformations to

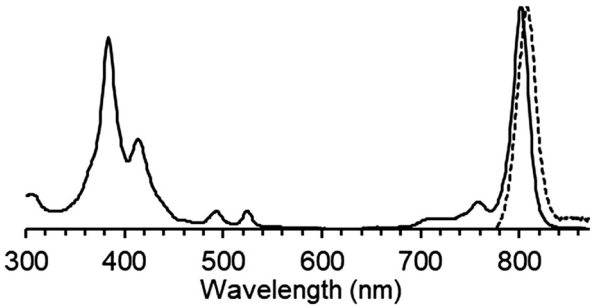

Fig. 1 Absorption (solid line) and fluorescence (dashed line; using 675 nm excitation) spectra of partially purified **BC-3** in CH_2Cl_2 at room temperature, normalized at the Q_y band.

give β,*meso*-phenalenobacteriochlorins. Compound **8** was converted (*via* intermediates **9**, **10** and **12**) into dihydrodipyrrin-acetal **13** following standard procedures[42] and use of an improved synthesis of Michael acceptor **11**.[71] The self-condensation of **13** with $BF_3{\cdot}OEt_2$ in MeCN[42] provided 5-unsubstituted bacteriochlorin **BC-4** in 41% yield, while with TMSOTf in the presence of 2,6-di-*tert*-butylpyridine (DTBP) in dichloromethane,[43] the reaction afforded the expected 5-methoxybacteriochlorin **BC-5** in 69% yield. Furthermore, **BC-4** and **BC-5** were converted[72] into the corresponding indium(III) and zinc(II) complexes **BC-6** and **BC-7** in 25% and 80% yield, respectively. Compound **8** was also converted (*via* intermediates **14** and **16–18**) through a recently reported Northern–Southern route[45] into dihydrodipyrrin-acetal **19** in 5 steps, making use of the known alkynoic acid **15**.[45] A single-crystal X-ray structure of **18** confirmed the integrity of the transformations (Fig. S1 and Table S1, ESI†). Compound **19** is a positional isomer of **13**. Treatment of **19** with TMSOTf/DTBP gave 10-methoxybacteriochlorin **BC-8** in 44% yield.

Oxidation of dinaphthylbacteriochlorins **BC-4–7** with DDQ or $FeCl_3$, which are common oxidizing agents in the synthesis of annulated porphyrins,[7,8] did not afford the expected annulated bacteriochlorins (Scheme 4A and Table S2, ESI†). The In(III) chelate **BC-6** and divalent Zn(II) chelate **BC-7** were created to probe whether metalation might facilitate the annulation process, either directly or upon subsequent macrocycle oxidation. It was straightforward to attribute the failure of annulation of these cases to steric interactions of the naphthalene units at the 2,12-positions with the *gem*-dimethyl groups at the 8,18-positions (Scheme 4B). Thus, similar oxidative annulation of **BC-8** and known bacteriochlorin **BC-9**,[45] wherein the *gem*-dimethyl groups are positioned away from the expected reaction sites, was attempted (Scheme 4C). However, neither β-to-*meso* nor *meso*-to-β oxidative annulation was observed with bacteriochlorins **BC-8** and **BC-9** (Tables S2 and S3, ESI†); similar attempts to annulate *meso*-naphthyldihydrodipyrrinatoboron complexes[73] also were unsuccessful (Table S4, ESI†).

Synthesis of β,*meso*-annulated bacteriochlorins *via* intramolecular direct arylation

Next, we focused on palladium-catalyzed intramolecular arylation as a means to gain access to β,*meso*-annulated bacteriochlorins. Unlike the unsubstituted naphthyl groups for the oxidative coupling as described above, halogen-substituted naphthyl groups are required for such direct arylation processes. Because avoidance of the steric hindrance of *gem*-dimethyl groups still appeared warranted, the Northern–Southern route[45] was adopted to prepare the bacteriochlorin.

The Northern–Southern route relies on the Pd-mediated coupling of an iodopyrrole and an alkynoic acid; hence, we planned to install a second halogen (bromide) at the β-pyrrole position in a subsequent reaction. The reaction of 4-carboethoxy-2-iodopyrrole[45] and 2,2-dimethylpent-4-ynoic acid under slightly modified conditions afforded known lactone-pyrrole **20**[45] in improved yield (80%, Scheme 5).[73] Electrophilic bromination of a pyrrole generally occurs at the α-position. Indeed, as shown in entry 1 of Table 1, treatment of **20** with *N*-bromosuccinimide (NBS, 1 equiv.) in DMF gave β-bromopyrrole **21** (minor, 18%) and α-bromopyrrole **22** (major, 50%). The structure of **21** was confirmed by X-ray crystallography (Fig. S2 and Table S5, ESI†). Upon screening of solvents, acetonitrile was found to show better β-selectivity (24% of **21** *versus* 17% of **22**, entry 2). The use of 2,4,4,6-tetrabromo-2,5-cyclohexadienone (TBCO)[74] as a brominating agent afforded a slightly increased amount of **21** (28%, entry 3). Addition of K_2CO_3 further improved the β-selectivity (31% of **21** and 19% of **22**, entry 4). Remarkably high β-selectivity was observed (50% of **21** and 6% of **22**, entry 5) when the reaction was carried out in the presence of K_2CO_3 and 2,4,6-tribromophenol (TBP), which is a coproduct from TBCO. After refinement of the reaction conditions, the yield of **21** reached 61% (entries 6–8). Interestingly, bromination by using NBS with TBP and K_2CO_3 resulted in low yields of **21** and **22** (entry 9). To the best of our knowledge, use of TBCO with TBP/K_2CO_3 represents a new condition for bromination. The origin of the β-selectivity caused by TBP/K_2CO_3 is unclear at present. Dihydrodipyrrin **23** was prepared from **21** by the established procedure[45] in 65% yield.

Attempted borylation of β-bromodihydrodipyrrin **23** proved fruitless (Table S6, ESI†). Compound **23** was converted into the corresponding difluoroboron- and dibutylboron-complexes[73] to thwart possible complexation of **23** with palladium upon direct benzo annulation, but this approach also was to no avail (Table S7, ESI†). Treatment of **23** with $Pd(OAc)_2$ in CH_2Cl_2 at room temperature[75] gave the bis(dipyrrinato)Pd(II) complex **24**, which did not survive attempted Suzuki coupling with 2-bromophenylboronic acid but instead reverted to **23**. Crystals of **24** suitable for X-ray analysis were obtained from vapor diffusion of hexanes into CH_2Cl_2/ethyl acetate solution at room temperature. For **24**, steric interaction between the pyrrolinyl methyl group of one dihydrodipyrrin and the α-hydrogen on the pyrrole ring of the other dihydrodipyrrin was observed in the single-crystal X-ray structural data (Fig. S3 and Table S8, ESI†).

At a minimum, the limitation in direct coupling highlights ongoing challenges associated with the synthetic chemistry of hydrodipyrrins despite extensive work.[45,47,76–79] Thus, the coupling reaction was carried out after the macrocycle formation. When oxidation of **23** with SeO_2 was performed in the absence of pyridine following the general procedure,[45] dihydrodipyrrin-acetal **25** was obtained in less than 27% yield following acetalization with trimethyl orthoformate.

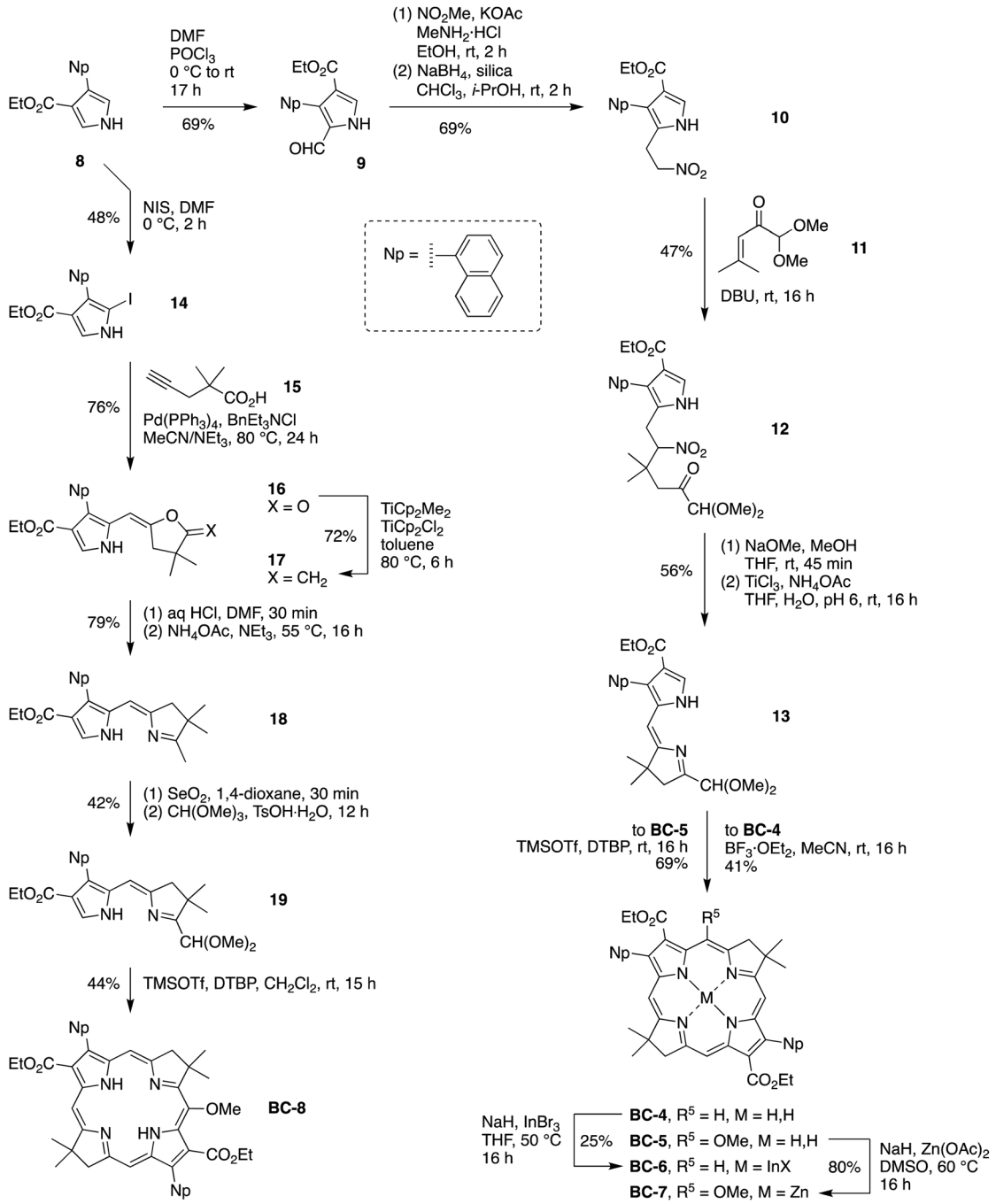

Scheme 3 Synthesis of di(1-naphthyl)bacteriochlorins **BC-4–8**.

Addition of pyridine to SeO_2 for the oxidation[80,81] improved the yield of **25** to 37%. Table 2 shows refinement of the conditions for the self-condensation of **25**. 1,2-Dichloroethane was found to be a better solvent than CH_2Cl_2 or $CHCl_3$ (Table S9, ESI†). When the concentration of **25** was 32 mM, the desired *meso*-unsubstituted bacteriochlorin **BC-10** was obtained in only 11% yield along with undesired *meso*-methoxybacteriochlorin **BC-11** in 52% yield (entry 1). Lower concentrations (5.0–18 mM, entries 2–6) tended to give increased **BC-10** (up to 32% in entry 4). Higher temperature was required for completion of the reactions at low concentrations (entries 3–6). Scaled-up reactions proceeded smoothly (entries 5 and 6). In prior studies with diverse dihydrodipyrrin-acetals,[43] the use of TMSOTf/DTBP tended to afford exclusively the *meso*-methoxybacteriochlorin. Here, both the *meso*-unsubstituted and *meso*-methoxy bacteriochlorin were obtained under these conditions regardless of temperature employed.

Suzuki–Miyaura cross-coupling of **BC-10** and excess (8-bromonaphthalen-1-yl)boronic acid (**26**) provided annulation precursor **BC-12** in 49% yield (Scheme 6). The molar ratio

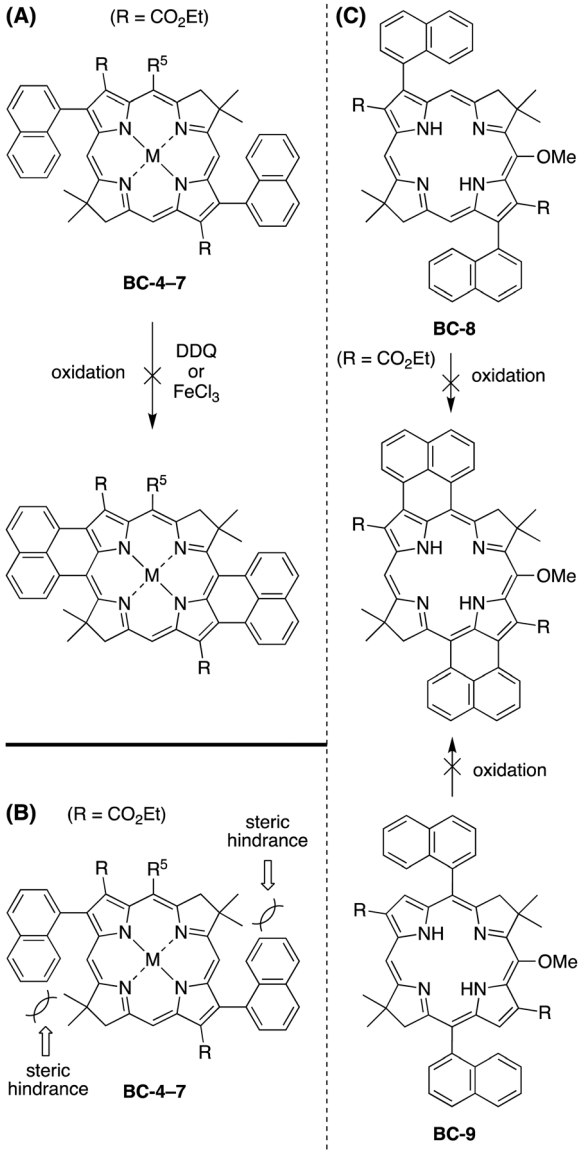

Scheme 4 Attempted oxidative annulation from (A) **BC-4–7** and (C) **BC-8** and **BC-9**. (B) Possible steric hindrance in **BC-4–7** during the oxidative annulation.

of bromoarylboronic acid **26** to bacteriochlorin **BC-10** was 10 : 1, giving 5 equiv. per bromo site on the bacteriochlorin. In this reaction, byproducts less polar than the bacteriochlorins, perhaps oligomerized aromatic rings, were observed by TLC analysis and readily removed by column chromatography. Compound **26**, reported previously but without characterization data,[82,83] was fully characterized here. NMR and TLC analysis indicated that **BC-12** was a mixture of two atropisomers (~1 : 1 ratio) attributed to hindered rotation of the bromonaphthyl groups at the 3- and 13-positions. Since both of the atropisomers should afford the same annulated compound, **BC-12** was used as the mixture in the next step. Palladium-catalyzed intramolecular direct arylation of **BC-12** afforded target β,*meso*-bis(phenaleno)bacteriochlorin **Phen-BC** in 37% yield. The ligand SPhos was found to be better than other ligands screened ($PCy_3{\cdot}HBF_4/K_2CO_3$ and $P^tBu_3{\cdot}HBF_4/K_2CO_3$).

In this synthetic strategy, the aromatic rings for annulation can be altered by changing the coupling partner of the Suzuki–Miyaura coupling. Thus, we also aimed for β-to-*meso* annulation with benzene rings by reaction of **BC-10** and (2-bromophenyl)-boronic acid (**27**), affording bis(2-bromophenyl)bacteriochlorin **BC-13** in 85% yield. Similar to **BC-12**, bacteriochlorin **BC-13** was isolated as a mixture of two atropisomers. Subsequent palladium-mediated arylation gave the desired β,*meso*-dibenzobacteriochlorin **Benz-BC** in 80% yield. In this case, PCy_3 gave a better result than that of SPhos. The NMR chemical shifts of the inner N–H protons of diverse synthetic bacteriochlorins are typically observed around −2 ppm in $CDCl_3$. In contrast, those of **Phen-BC** and **Benz-BC** were found at 1.97 and 2.89 ppm, respectively, suggesting unusual ring currents in the annulated macrocycles.

Photophysical properties

Fig. 2 shows absorption spectra for the two new annulated bacteriochlorins along with several reference compounds, all of which contain 8,18-geminal dimethyl groups to stabilize the bacteriochlorin. The Q_y band for **Benz-BC** (1033 nm) lies 120 nm to longer wavelength than that for **Phen-BC** (913) nm, which in turn is bathochromic from those for diimide **I2-BC** (875 nm),[5] monoimide **I-BC** (818 nm),[6] diester **Es-BC** (753 nm)[84] and parent **H-BC** (713 nm).[85] The structures of **I2-BC** and **I-BC** are shown in Chart 2 whereas **H-BC** and **Es-BC** are shown in Chart 3. Fig. 2 also shows fluorescence spectra. The Q_y fluorescence maximum is bathochromically shifted from the Q_y absorption peak by 4–9 nm (65–84 cm^{-1}) for all constructs except for **Phen-BC**, which shows a considerably larger Stokes shift of 20 nm (235 cm^{-1}). The emission band for **Phen-BC** is also broader (49 nm, 586 cm^{-1}) than that of the other bacteriochlorins (12–34 nm; 230–346 cm^{-1}). The spectral characteristics are given in Table 3.

The fluorescence quantum yield (Φ_f) of **Benz-BC** is estimated to be very small ($\sim 3 \times 10^{-5}$) and that for **Phen-BC** is somewhat larger but also low (0.004). Both annulated bacteriochlorins are less fluorescent than diimide **I2-BC** (0.027) and monoimide **I-BC** (0.064), which themselves are weak emitters. In turn, all of these constructs, which employ *exo*-macrocycle connectivity between adjacent *meso* and β-pyrrole positions, have much smaller Φ_f values than benchmark bacteriochlorins **Es-BC** and **H-BC** (0.13–0.14; Table 3). The lifetime (τ_s) of the lowest singlet excited state (S_1) shows a similar pattern (Table 3): **Benz-BC** (7 ps) < **Phen-BC** (150 ps) < **I2-BC** (0.98 ns) < **I-BC** (1.9 ns) < **Es-BC** (3.3 ns) < **H-BC** (3.8 ns). As will be discussed below, the weak fluorescence and short S_1 lifetimes for the annulated bacteriochlorins cannot be attributed solely to a lower excited-state energy than the benchmarks.

The S_1 lifetimes noted above were measured by transient absorption (TA) spectroscopy, and in some cases also by time-resolved fluorescence. The TA studies also give insight into yields of the $S_1 \rightarrow T_1$ intersystem crossing and $S_1 \rightarrow S_0$ internal conversion pathways that compete with $S_1 \rightarrow S_0$ fluorescence.

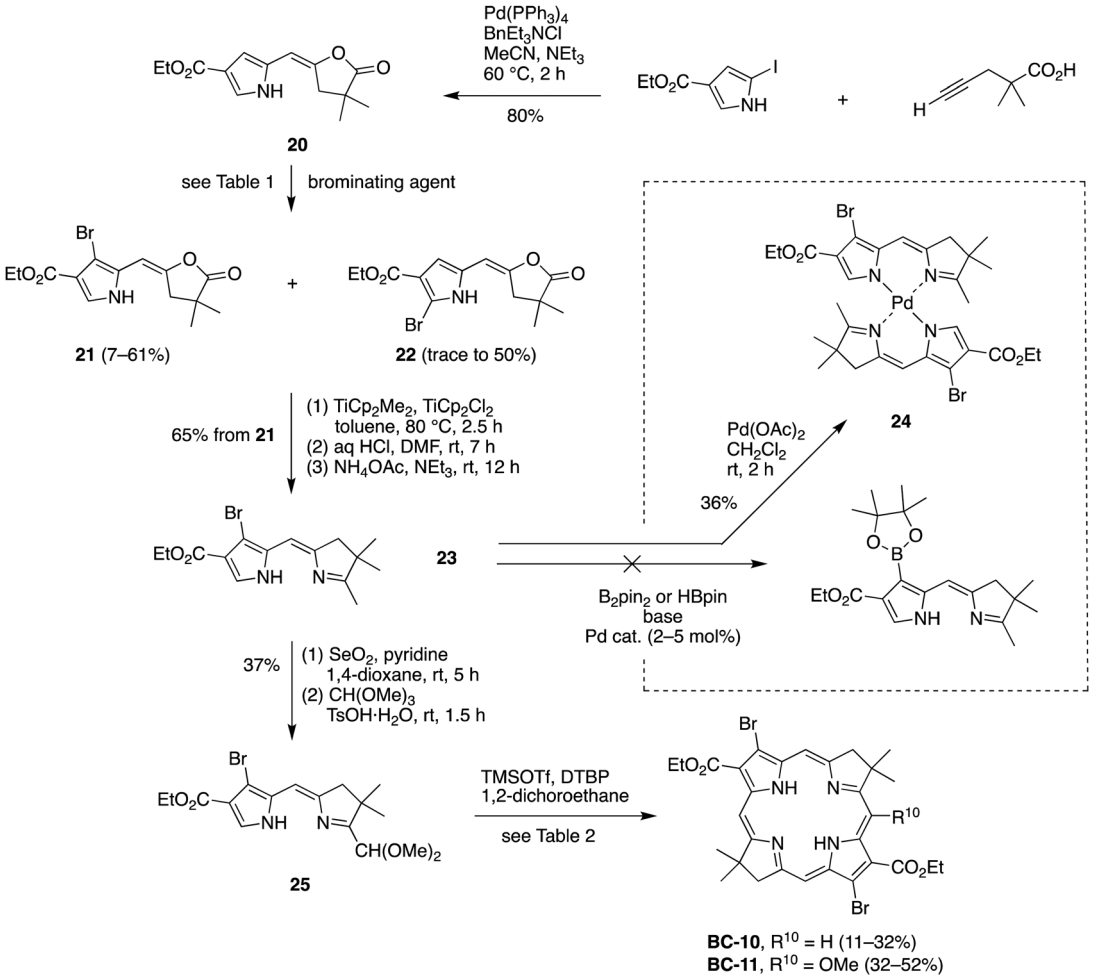

Scheme 5 Synthesis of bromodihydrodipyrrin **23** en route to dibromobacteriochlorin **BC-10**.

Table 1 Bromination of lactone-pyrrole **20**

20 —brominating agent→ **21** + **22**

Entry	Brominating agent (equiv.)	Solvent	Additive (equiv.)	Recovered **20**[a] (%)	**21**[a] (%)	**22**[a] (%)
1[b]	NBS (1)	DMF	None	—[c]	18[d]	50[d]
2[e]	NBS (1)	MeCN	None	—[c]	24[d]	17[d]
3[f]	TBCO (1)	MeCN	None	16	28	31
4[f]	TBCO (1)	MeCN	K_2CO_3 (1)	23	31	19
5[f]	TBCO (1)	MeCN	TBP (1), K_2CO_3 (1)	23	50	6
6[f]	TBCO (1)	MeCN	TBP (1), K_2CO_3 (2)	25[d]	53[d]	9
7[f]	TBCO (1)	MeCN	TBP (2), K_2CO_3 (3)	26	49	5
8[f]	TBCO (1.6)	MeCN	TBP (2), K_2CO_3 (3.6)	Trace	61[e]	Trace
9[f]	NBS (1)	MeCN	TBP (2), K_2CO_3 (3)	49	7	3

[a] Calculated from ^{1}H NMR spectroscopic analysis by using 2-nitromesitylene as an internal standard unless otherwise noted. [b] The reaction was carried out at −20 °C to r.t. for 10 h. [c] Not determined. [d] Isolated yields. [e] The reaction was carried out at 0 °C to r.t. for 1.5 h. [f] The reactions were carried out at 0 °C for 1 h.

Representative TA data for the two annulated bacteriochlorins is given in Fig. 3. The TA difference spectrum for **Phen-BC** (Fig. 3A) at 0.4 ps after a 0.1 ps excitation flash is dominated by a feature at ~930 nm that is comprised of bleaching of the ground state $S_0 \rightarrow S_1$ absorption band along with $S_1 \rightarrow S_0$ stimulated emission. During the next tens of picoseconds, there are minor spectral changes that can be attributed to relaxations (vibrational, solvent, *etc.*) in the excited state. Subsequently, the prominent 930 nm feature and the rest of the spectrum diminish uniformly to almost $\Delta A = 0$ by about 2 ns, reflecting decay of the S_1 excited state with a time constant of 150 ps (Fig. 3B). Close examination of the data to 7 ns indicates

Table 2 Yields of **BC-10** and **BC-11** under different reaction conditions

25 —self-condensation→ **BC-10** + **BC-11**

Entry[a]	Conc. (mM)	Temp.	Time (h)	**BC-10**[b] (%)	**BC-11**[b] (%)
1	32	r.t.	20	11	52
2	18	r.t.	20	15	32
3	10	60 °C	4	29	37
4	5.6	Reflux	7	32	38
5[c]	5.6	Reflux	8	31	39
6[d]	5.0	Reflux	11	29	36

[a] All reactions were carried out with TMSOTf (7.5 equiv.) and DTBP (30 equiv.) in 1,2-dichloroethane on a 0.12 mmol scale unless otherwise noted. [b] Isolated yields. [c] The reaction was carried out on a 0.71 mmol scale. [d] The reaction was carried out on a 2.00 mmol scale.

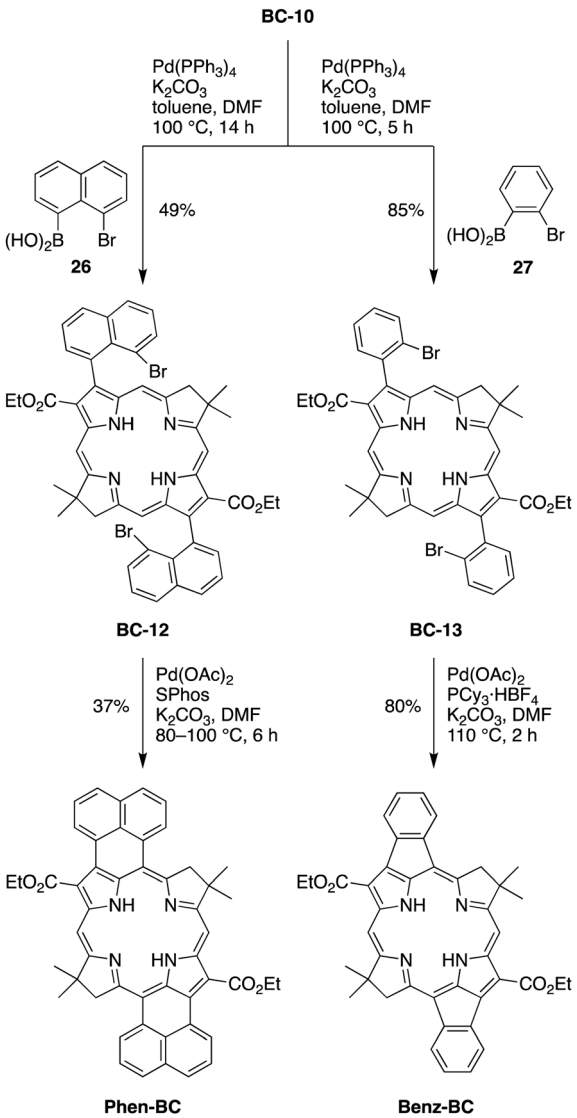

Scheme 6 Synthesis of β,*meso*-annulated bacteriochlorins **Phen-BC** and **Benz-BC**.

that a very small amount of Q_y bleaching remains that corresponds to about 2% of the bleaching at early times. This small

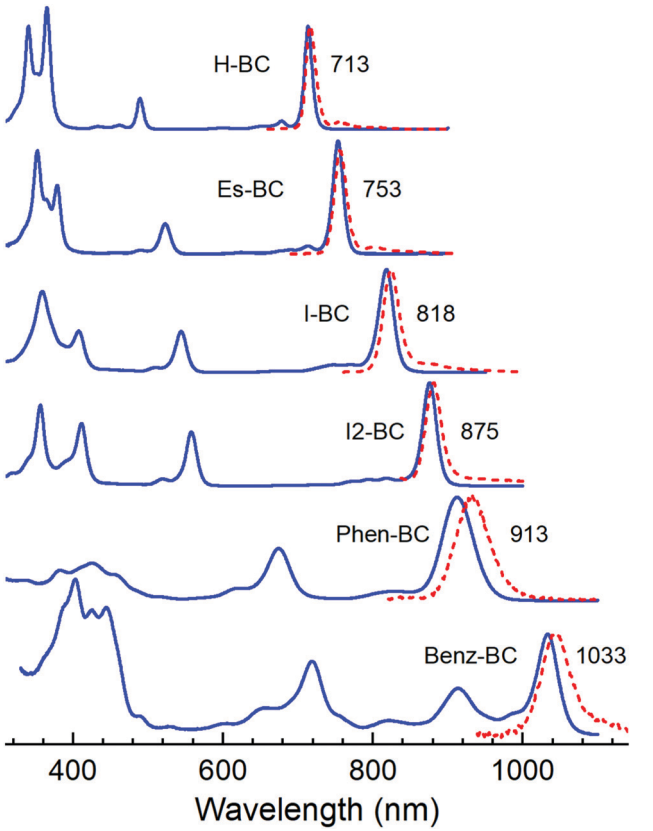

Fig. 2 Absorption spectra (blue) and fluorescence spectra (red) of the annulated bacteriochlorins **Phen-BC** and **Benz-BC** and known reference compounds. The absorption spectra are normalized to the Q_y maximum. The emission spectra were obtained using excitation in the Q_x band (490, 522, 544, 557, 675, and 715 nm, respectively); for each compound the same spectrum was obtained using excitation in the Soret band.

asymptotic signal likely represents the lowest triplet excited state (T_1), which forms from S_1 with a yield of $\Phi_{isc} = 0.02$. Given this value and $\Phi_f = 0.004$ for **Phen-BC**, the yield of $S_0 \rightarrow S_1$ internal conversion is $\Phi_{ic} = 0.98$.

The analogous TA data for **Benz-BC** are dominated by a spectral feature at ~1030 nm (Fig. 3C) that disappears with a time constant of 7 ps (Fig. 3D), which reflects the S_1 lifetime. At long times, the Q_y bleaching is less than 1% of the initial value, reflecting essentially no formation of the T_1 excited state. Given the extremely small Φ_f value (<0.0001), this means that decay of the S_1 excited state of **Benz-BC** occurs 99% by $S_0 \rightarrow S_1$ internal conversion (Table 3).

Molecular orbital characteristics and calculated spectral properties

The energies and electron density distributions calculated by DFT for the frontier MOs of **Es-BC**, **Phen-BC**, and **Benz-BC** are shown in Fig. 4. For benchmark **Es-BC** (Fig. 4A), the two highest occupied molecular orbitals (HOMO and HOMO−1) and the two lowest unoccupied molecular orbitals (LUMO and LUMO+1) have the familiar electron-density distributions of the frontier MOs of Gouterman's four-orbital model for tetrapyrrole chromophores.[87–89] In this model, linear combinations of excited-state

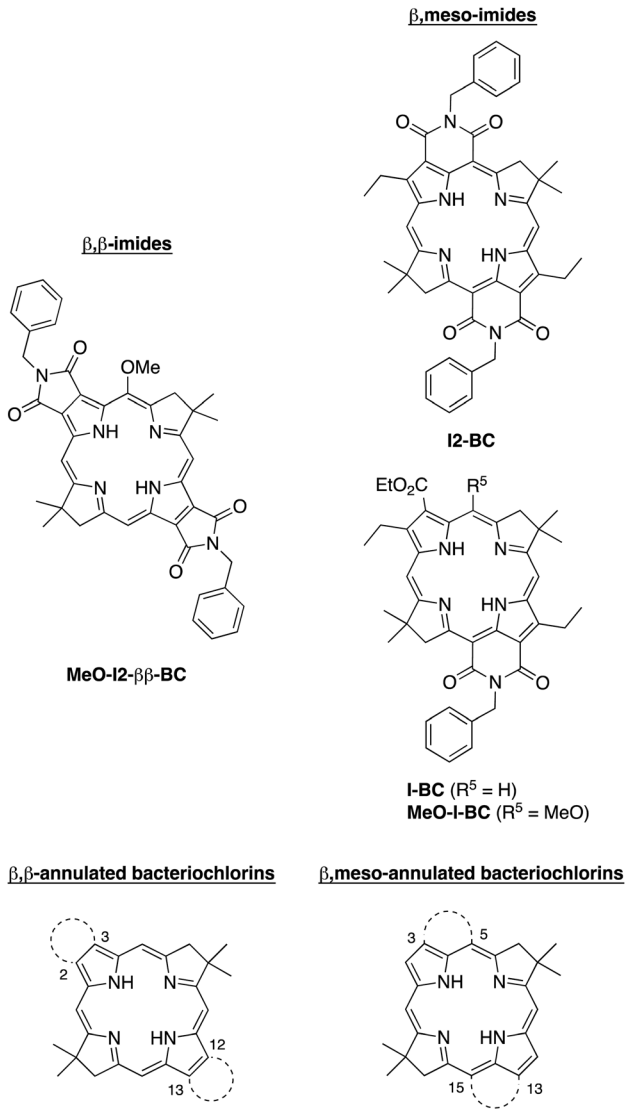

Chart 2 Structures of bacteriochlorins bearing β,β- or β,*meso*-imides[5,6] and bacteriochlorins with β,β- or β,*meso*-annulated aromatic hydrocarbons.

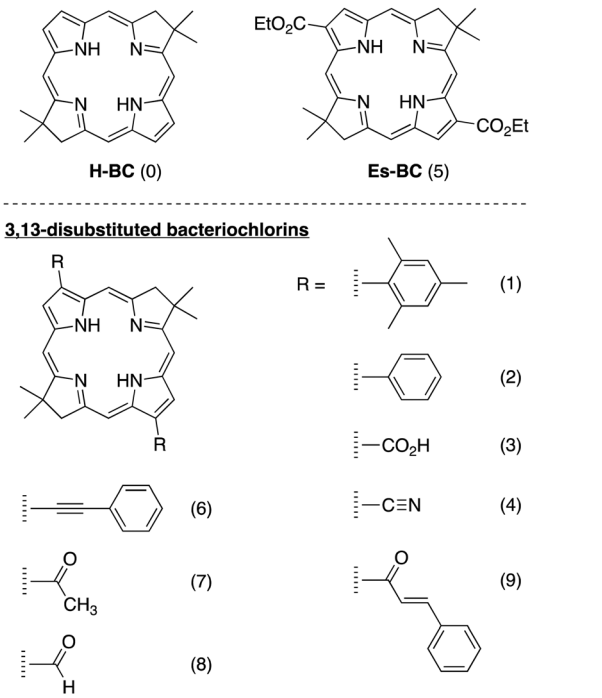

Chart 3 Bacteriochlorin benchmarks.[5,6,84–86] The numbers in parentheses identify the data points in the energy-gap plot (*vide infra*).

configurations derived from one-electron promotions among the four orbitals dominate the spectral properties of the molecules. The HOMO is the $a_{1u}(\pi)$-like orbital (using D_{4h} nomenclature), the HOMO−1 is $a_{2u}(\pi)$-like and LUMO and LUMO+1 are akin to $e_{gx}(\pi^*)$ and $e_{gy}(\pi^*)$. Also shown in Fig. 4 are the next two filled orbitals (HOMO−2 and HOMO−3) and next two empty orbitals (LUMO+2 and LUMO+3). The four frontier MOs (HOMO−1 through LUMO+1) of **Phen-BC** (Fig. 4B) and **Benz-BC** (Fig. 4C) are generally similar to those for **Es-BC** but show significant electron density delocalized onto the annulated rings for certain orbitals. This delocalization is equally or more pronounced for the HOMO−3, HOMO−2, LUMO+2 and LUMO+3, which show additional characteristics that differ from those from the benchmark.

At the lower left of each of the three main panels of Fig. 4 are the transition dipole moment directions for absorption from the ground state to several singlet excited states. The directions are obtained from TDDFT calculations. For **Es-BC**, the transition from S_0 to S_1 (Q_y) is along the axis that contains the N–H bonds (the *y*-axis) and the transition to S_2 (Q_x) is essentially perpendicular to that. The S_1 transition is also along the *y*-axis for **Phen-BC**, but the S_2 transition is notably rotated off the *x*-axis. In comparison, the S_2 transition for **Benz-BC** is approximately *x*-polarized, and the S_1 transition is mainly *y*-polarized but rotated somewhat off the *y*-axis and directed toward the annulated rings.

Additional results of the TDDFT calculations are given in Fig. 5–7 for **Es-BC**, **Phen-BC** and **Benz-BC**, respectively. Each figure compares the measured absorption spectrum (brown) with one calculated by TDDFT shown as sticks and an associated line plot in which calculated transitions are given Gaussian skirts (dashed blue). The calculations for all three molecules reproduce the Q_y band ($S_0 \rightarrow S_1$) in the NIR, the Q_x band ($S_0 \rightarrow S_2$) in the red-green, and nominal B_x ($S_0 \rightarrow S_3$) and B_y ($S_0 \rightarrow S_4$) bands in the blue-violet (Soret) region. The calculations also reproduce the observed bathochromic shift of the Q_y band in progressing from **Es-BC** to **Phen-BC** to **Benz-BC**, and for the two annulated molecules, place one additional transition in the Soret region that carries significant oscillator strength and is located between the nominal B_x and B_y bands. This latter prediction can be seen by examining the percent contribution of the various one-electron promotions to the transitions (*e.g.* HOMO → LUMO, HOMO−1 → LUMO+1), which are given in Tables S10–S12 (ESI†).

The energies of the various primary, *i.e.* (0,0), transitions of **Es-BC**, **Phen-BC**, and **Benz-BC** are reasonably well reproduced by the TDDFT calculations; however, the relative intensities of certain transitions differ appreciably from those observed. Of particular note is the disparity in the observed (relatively weak)

Table 3 Photophysical data[a]

Compound	Q_y abs (nm)	Q_y em (nm)	FWHM abs (cm^{-1})	Δ^b abs-em (cm^{-1})	$S_1{}^c$ energy (eV)	τ_s (ns)	Φ_f	Φ_{isc}	Φ_{ic}	$(k_f)^{-1}$ (ns)	$(k_{isc})^{-1}$ (ns)	$(k_{ic})^{-1}$ (ns)
Benz-BC	1033	1042	321	84	1.20	0.007	2×10^{-5}	≤ 0.01	0.99	35	—	0.01
Phen-BC	913	933	586	235	1.34	0.15	0.004	0.02	0.98	38	7.5	0.15
I2-BC[d]	875	880	278	65	1.41	0.98	0.027	0.18	0.79	36	5.4	1.2
I-BC[e]	818	823	346	74	1.51	1.9	0.064	0.51	0.43	30	3.7	4.4
BC2[f]	818	838	594	292	1.50	1.6	0.14	0.31	0.55	11	5.2	2.9
Es-BC[g]	753	758	286	88	1.64	3.3	0.13	0.56	0.31	25	8	11
H-BC[h]	713	717	230	78	1.73	3.8	0.14	0.63	0.23	27	6.5	17

[a] Data were acquired in toluene at room temperature. [b] Stokes shift between the Q_y absorption and fluorescence maxima. [c] Average energy of the Q_y absorption and fluorescence maxima. [d] From ref. 5. [e] From ref. 6. [f] Static absorption and fluorescence data as well as TA spectra are available (Fig. S4 and S5, ESI). [g] From ref. 84. [h] From ref. 85.

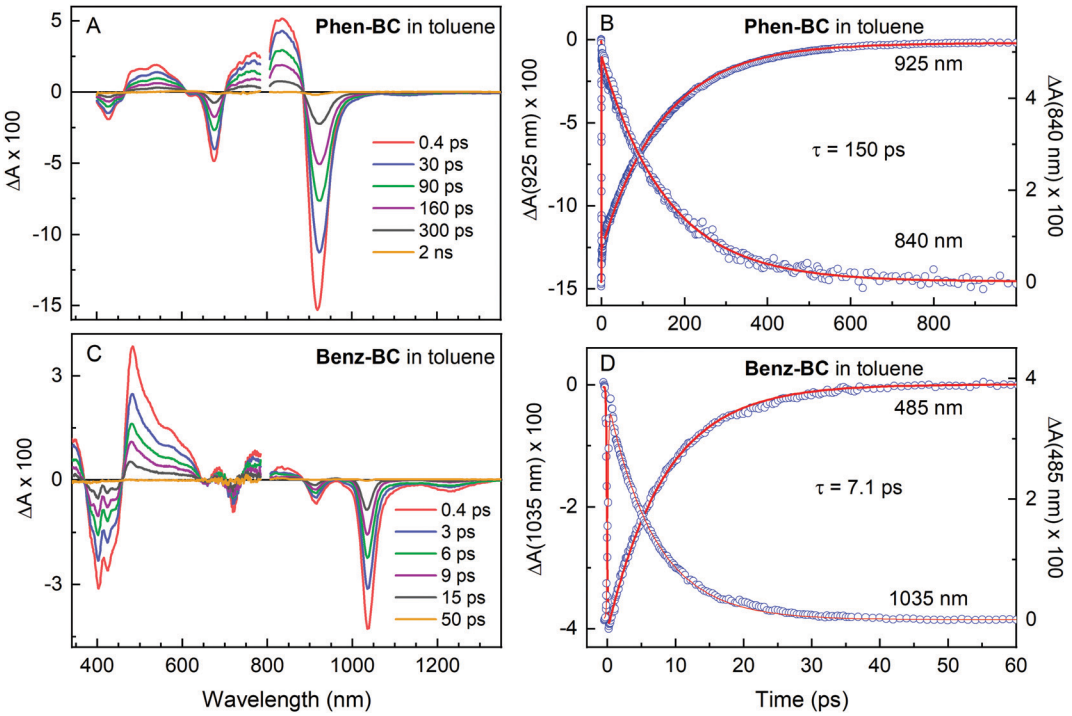

Fig. 3 Transient absorption data for **Phen-BC** excited at 715 nm (A and B) and **Benz-BC** excited at 675 nm (C and D) in toluene obtained using 100 fs flashes.

versus calculated (relatively strong) features in the Soret region for **Phen-BC**. We also note that TDDFT does not include prediction of vibronic transitions, *i.e.* (1,0), (2,0), *etc.*, which are clearly visible to the blue of the $Q_y(0,0)$ and/or $Q_x(0,0)$ bands for all three molecules. The band of **Benz-BC** at ~913 nm, which exhibits an energy consistent with a $Q_y(1,0)$ vibronic satellite, is unusually intense for a tetrapyrrole-related molecule and could easily be mistaken for a primary band. The influence of the vibronic features of the annulated bacteriochlorins on the photophysical properties will be addressed further below.

Fig. 5–7 also give the natural transition orbitals (NTOs) for each calculated transition. The construction of these orbitals takes into account the contributing configurations to give the net electron-density distributions of the occupied orbital and the virtual (empty) orbital as if a single one-electron promotion were involved.[90] The NTOs provide a more physically meaningful picture of the electron density change involved in an optical transition than can be gleaned from the orbitals themselves. Ideally, the contributions from various configurations should be distilled down into one pair of NTOs (filled and empty) for a given transition. However, for all three molecules for which TDDFT calculations were performed here (**Es-BC**, **Phen-BC** and **Benz-BC**) two pairs of NTO promotions are involved, with relative contributions indicated by the eigenvalues (from analysis of the transition density matrices) given in Fig. 5–7. This points to the underlying complexity and that both pairs of NTOs should be taken into account in assessing the net electron-density change accompanying the transition.

The situation is relatively straightforward for benchmark **Es-BC** (Fig. 5). The S_1 (Q_y) transition is comprised mainly (~90%) of a promotion between an $a_{1u}(\pi)$-like filled NTO to an $e_{gx}(\pi^*)$-like empty NTO and a small (~10%) contribution

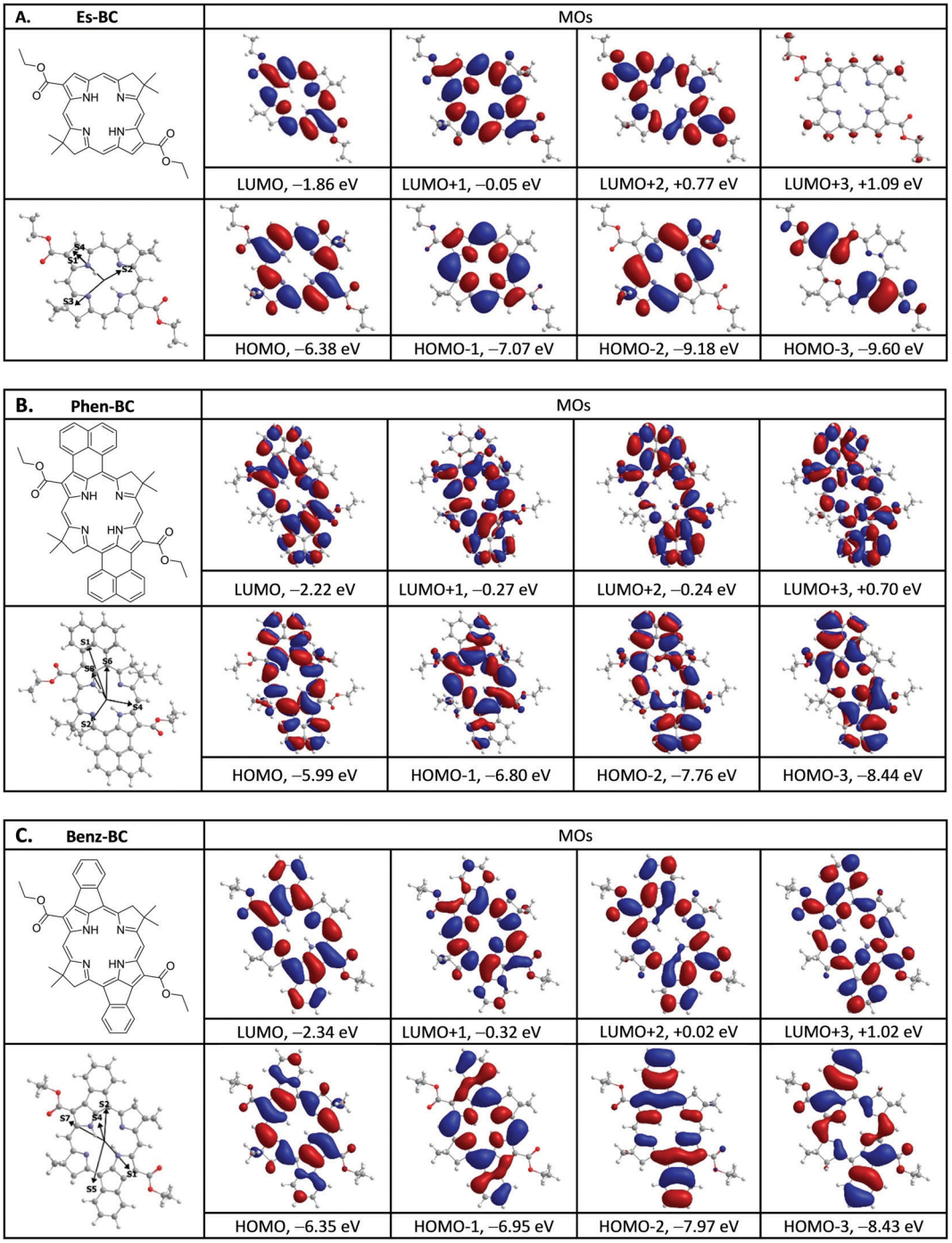

Fig. 4 Structure, transition-dipole directions for absorption from S_0 to excited states that carry significant oscillator strength in the near-UV to NIR regions (S_1, S_2, *etc.*), and frontier MOs for **Es-BC** (A), **Phen-BC** (B) and **Benz-BC** (C).

from $a_{2u}(\pi)$-like NTO to an $e_{gy}(\pi^*)$-like NTO. On the other hand, the S_4 (B_y) transition has the reverse contributions. The compositions of these two *y*-polarized transitions are consistent with expectations based on the four-orbital model. Similarly, the S_2 (Q_x) and S_3 (B_x) transitions are comprised of mixtures of promotions between an $a_{1u}(\pi)$-like filled NTO to an $e_{gy}(\pi^*)$-like empty NTO and between an $a_{2u}(\pi)$-like NTO to an $e_{gx}(\pi^*)$-like NTO. Examination of the NTOs for the **Phen-BC** (Fig. 6) and **Benz-BC** (Fig. 7) show some of the same characteristics, modified or supplemented by effects of electron delocalization onto the annulated rings.

Discussion

Synthesis

While numerous β,β- and β,*meso*-annulated porphyrins are known,[7,8] hardly any such bacteriochlorins have heretofore

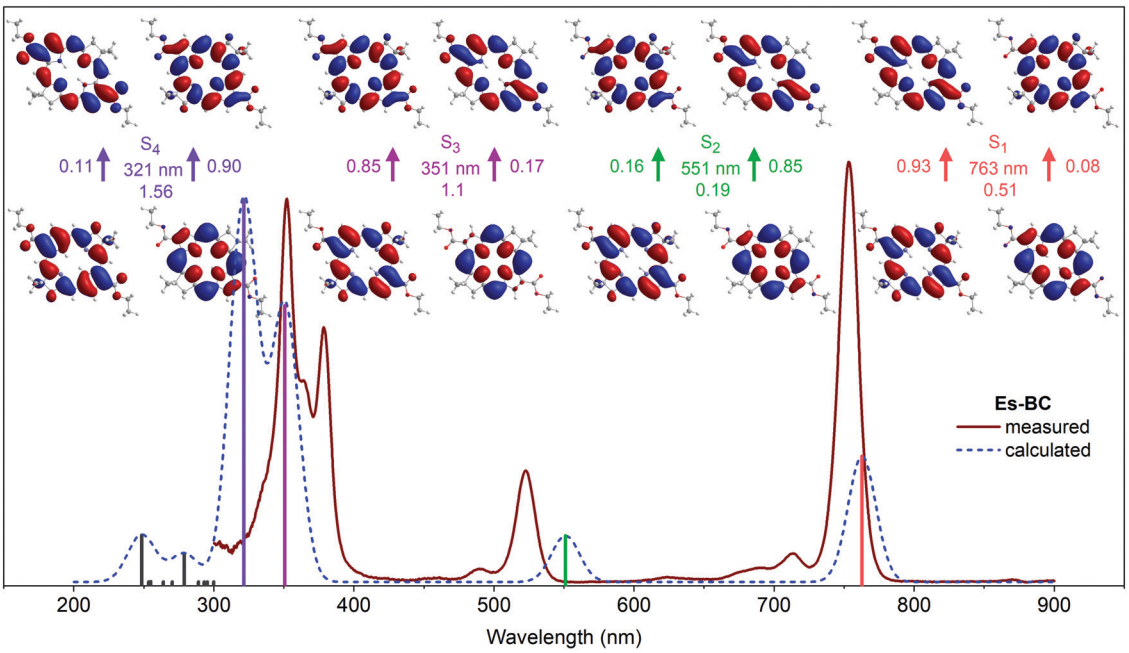

Fig. 5 Comparison for **Es-BC** of the absorption spectra in toluene that are measured (brown line) or calculated *via* TDDFT (dashed blue lines and colored sticks) normalized at the highest peak. Calculated spectral features were given 10 nm Gaussian skirts. Shown for the lowest four transitions (S_0 to S_1–S_4) are the natural transition occupied and virtual orbitals (NTOs) along with the wavelength and oscillator strength of the transition obtained from TDDFT. Two NTO promotions contribute to each transition, with weights (eigenvalues) indicated by the values that flank the arrows.

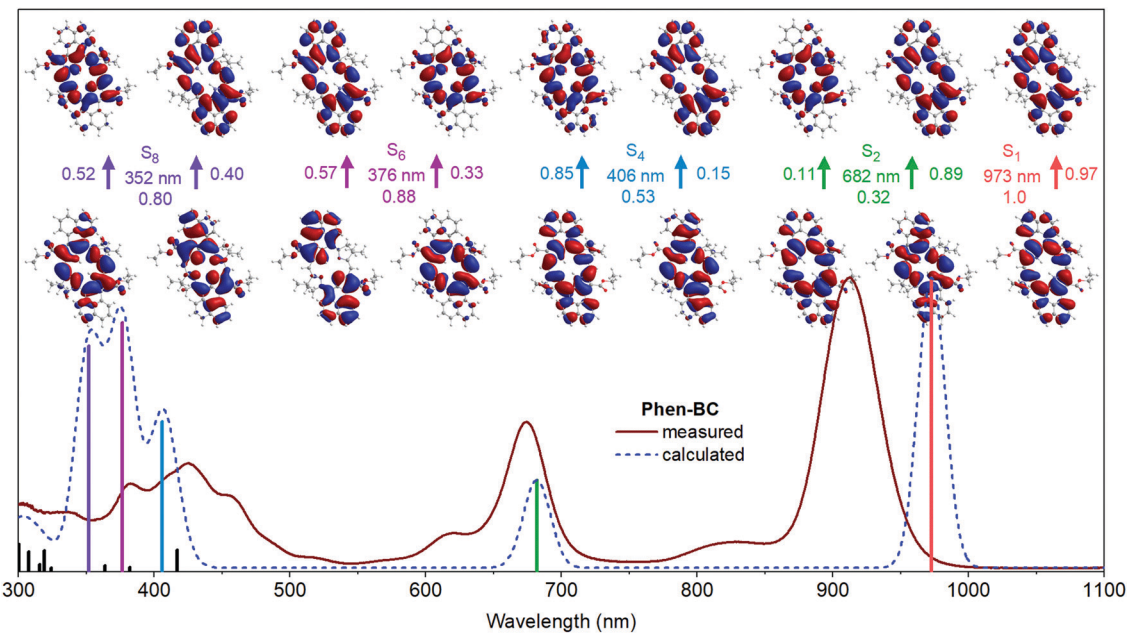

Fig. 6 Comparison for **Phen-BC** of the absorption spectra in toluene that are measured (brown line) or calculated *via* TDDFT (dashed blue lines and colored sticks) normalized at the highest peak. Calculated spectral features were given 10 nm Gaussian skirts, except for $S_0 \rightarrow S_1$ and $S_0 \rightarrow S_2$, which were set at 20 nm. Shown for the lowest five transitions that carry significant oscillator strength (S_0 to S_1, S_2, S_4, S_6, and S_8) are the natural transition occupied and virtual orbitals (NTOs) along with the wavelength and oscillator strength of the transition obtained from TDDFT. Two NTO promotions contribute to some transitions, with weights (eigenvalues) indicated by the values that flank the arrows.

been synthesized. The finding that the established routes to porphyrins[7–33] were largely unsuited, at least in our hands, was a surprise, although we were aware of other reactivity differences of bacteriochlorins *versus* porphyrins. The chemistry of dihydrodipyrrins[45,47,76–79] also differs considerably from that of dipyrrins, where annulation has been achieved *via* several means.[91] We explored 7 distinct routes to the annulated bacteriochlorins. The routes to β,β-annulated bacteriochlorins

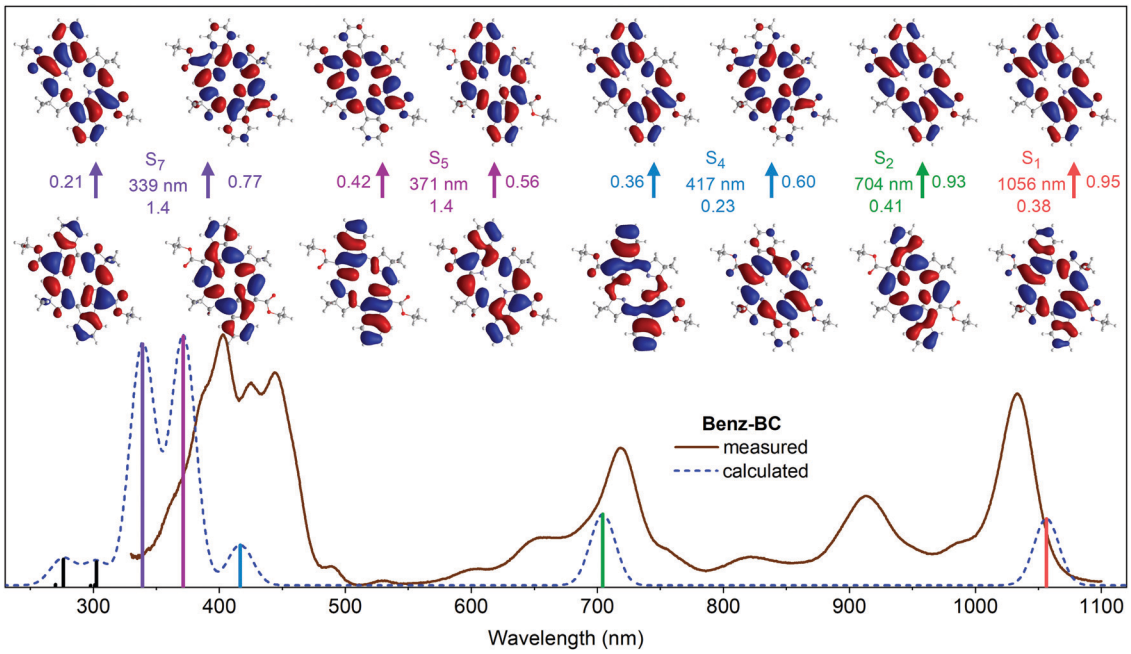

Fig. 7 Comparison for **Benz-BC** of the absorption spectra in toluene that are measured (brown line) or calculated *via* TDDFT (dashed blue lines and colored sticks) normalized at the highest peak. Calculated spectral features were given 10 nm Gaussian skirts. Shown for the lowest five transitions that carry significant oscillator strength (S_0 to S_1, S_2, S_4, S_5, and S_7) are the natural transition occupied and virtual orbitals (NTOs) along with the wavelength and oscillator strength of the transition obtained from TDDFT. Two NTO promotions contribute to some transitions, with weights (eigenvalues) indicated by the values that flank the arrows.

include cyclization of adjacent appended methyl acrylate units (Scheme 1), synthesis beginning with annulated pyrroles (*i.e.*, isoindoles, Scheme 2) and use of a non-conjugated β,β-annulated pyrrole (*i.e.*, a tetrahydroisoindole). The routes to β,*meso*-annulated bacteriochlorins include oxidative cyclization of an appended β- or *meso*-substituent on the bacteriochlorin (Scheme 3), cyclization of an appended β- or *meso*-substituent on a dihydrodipyrrin (Scheme 5), and ultimately the successive Pd-catalyzed arylation shown in Scheme 6. Extensive information, procedures and accompanying literature concerning attempted routes are provided in the ESI† (Schemes S1–S10). Some subtleties of the syntheses warrant comment. In particular, the question may arise why two successive Pd-couplings are employed to install the β,*meso*-annulation as opposed to pre-installation of, say, a bromoaryl group in the beginning of the synthesis at the pyrrole stage.

β-Aryl groups are carried through the synthesis very successfully, as exemplified by the naphthyl group in Scheme 3. Scheme 3 shows two routes to dinaphthyl-diester bacteriochlorins, which differ (1) in the positions of the substituents relative to the position of the *gem*-dimethyl groups and the unfettered *meso*-position, (2) the means of creating the dihydrodipyrrin precursors, and (3) the position of the *gem*-dimethyl groups relative to the pyrrole. The bacteriochlorins with the naphthyl groups at the 2,12-positions (**BC-4–7**) were constructed with the longstanding "Eastern–Western" route,[42] whereas those at the preferred 3,13-positions (**BC-8,9**) were constructed with the more recent "Northern–Southern" route.[45] The successful annulations (Scheme 6) were achieved with bacteriochlorins (**BC-12,13**) resembling **BC-8,9** in substituent patterns. A present limitation of the Northern–Southern route is the requirement for a Pd-catalyzed coupling of an iodopyrrole and an alkynoic acid to construct the pyrrole-lactone leading to the dihydrodipyrrin. The first Pd-coupling in the annulation in Scheme 6 uses a 5-fold excess of the bromoarylboronic acid *versus* the bromo sites on the bacteriochlorin with acceptable yields (49%, 85%) on the basis of the limiting bacteriochlorin. Such an excess of a β-bromoaryl-substituted iodopyrrole would be far less practical at the start of a Northern–Southern synthesis. In principle, the same substitution pattern could be created *via* the Eastern–Western route, but additional steps would be required to access the requisite 2-formyl-3-ethoxycarbonyl-4-(bromonaphthyl)pyrrole. In summary, the studies here have achieved the synthesis of β,*meso*-annulated bacteriochlorins yet at the same time have highlighted significant unresolved limitations in bacteriochlorin chemistry.

Photophysical features

The trends in the absorption spectral positions among the two new annulated bacteriochlorins and several benchmark bacteriochlorins are reproduced by the TDDFT calculations. **Phen-BC** basically has a naphthalene unit fused with the macrocycle, and the Q_y band is at 933 nm. **Benz-BC** basically has a benzene unit fused with the macrocycle, and the Q_y band is at 1033 nm. The two annulated bacteriochlorins thus absorb at the low-energy edge of the first NIR region (~700–1000 nm) and the high-energy edge of the second NIR region (1000–1700 nm),[92,93] respectively. If the excited-state energies and spectral positions

simply followed the particle-in-a-box model, one would have expected the larger **Phen-BC** to absorb at longer wavelength (lower energy) than **Benz-BC** because the S_1–S_0 energy gap is inversely proportional to the square of the box size. Examination of the energy gaps between the relevant orbitals involved in the Q_y transition (HOMO → LUMO and HOMO−1 → LUMO+1) suggests that the Q_y band of **Phen-BC** would be at lower energy than that for **Benz-BC**. However, the measured spectra show the opposite order and this is supported by the TDDFT calculations.

A factor that the calculations must effectively take into account, and which is also integral to the four-orbital model, is the configuration-interaction (CI) energy. This parameter is sensitive to the electron density distribution in the macrocycle. We have shown this from analysis of tetrapyrrole-based panchromatic absorbers, where the CI energy, and not simply the MO energy gaps, is a dominant factor in determining the spectral properties.[94] Thus, we speculate that annulation of the bacteriochlorin perturbs the CI energy sufficiently to complement effects on the MO energies in governing the observed spectra, and in particular the position of the Q_y band for the annulated bacteriochlorins. Spectral simulations using the four-orbital model support this conjecture.

The question arose as to whether the observed short excited-state (S_1) lifetime for **Phen-BC** and **Benz-BC** was simply a matter of the long-wavelength of absorption, and commensurate low energy level of the excited-state in each case. Fig. 8 plots the rate constant for $S_1 \rightarrow S_0$ internal conversion obtained from analysis of the TA data for the annulated bacteriochlorins studied here, the benchmark bacteriochlorins noted above (Table 3) and a host of other tetrapyrroles (Chart 3)[5,6,84–86] studied previously. The red line in Fig. 8 suggests that if **Phen-BC** and **Benz-BC** followed the normal energy-gap law for bacteriochlorins, the molecules would have much longer S_1 lifetimes than is observed. For example, one would have expected an S_1 lifetime of about 400 ps for **Benz-BC**, rather than the observed 7 ps. The blue line in Fig. 8 is a fit to the data for **Benz-BC**, **Phen-BC**, diimide **I2-BC**, and monoimides **I-BC** and **MeO-I-BC**, all of which have added connectivity (*via* fused conjugated motifs; see Chart 2) between nearby *meso* and β-pyrrole positions.[5,6] The correlation suggests that the annulated β-*meso* motif must introduce some factor to enhance nonradiative internal conversion in these constructs over normal bacteriochlorins. The development of chromophores with fluorescence at wavelengths >1000 nm is an active area of research.[95]

A potential source of enhanced internal conversion in the annulated (and imide) bacteriochlorins that employ β-*meso* connectivity can be gleaned from the optical spectra in Fig. 3. In particular, note the extraordinarily intense and broad $Q_y(1,0)$ band at ~913 nm for **Benz-BC**. The breadth suggests that there are likely a number of unresolved vibronic components, and the intensity indicates that there are modes coupling Q_y with higher energy states, such as B_y or perhaps Q_x. For the imides, particularly **I2-BC**, the peak intensity in the nominal $Q_y(1,0)$ region for that molecule (780–820 nm) is normal, but there is a ladder of small overlapping features that extend up toward the $Q_y(0,0)$ band. Thus, internal conversion may be enhanced in constructs that utilize conjugated β-*meso* connectivity either *via* vibronic (Herzberg–Teller) coupling or *via* improved Franck–Condon factors through better energy matching due to the contribution of multiple vibrational levels.

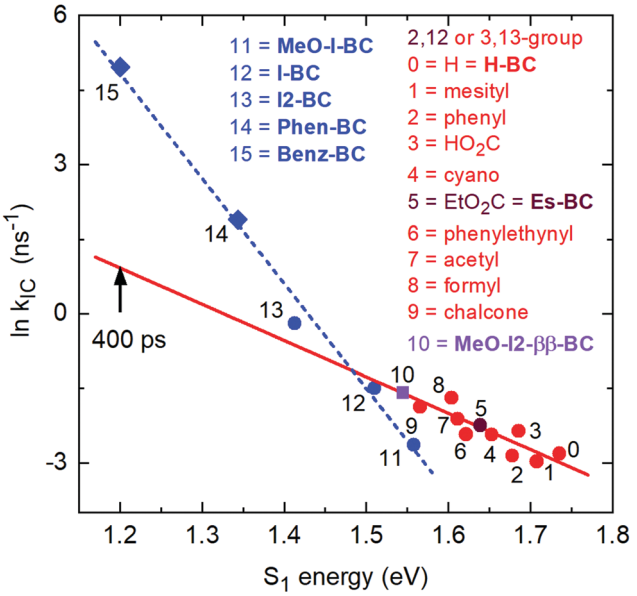

Fig. 8 Energy-gap law plot showing the natural logarithm of the rate constant for $S_1 \rightarrow S_0$ internal conversion *versus* the S_1 energy for various types of bacteriochlorins. The blue line is a fit for bacteriochlorins bearing one or two imide moieties or annulated rings spanning adjacent *meso* and β-pyrrole positions. The red line is a fit for the 10 benchmark bacteriochlorins from Chart 3 (and one β,β-annulated bis(imide)bacteriochlorin, from Chart 2). The latter line projects an S_1 lifetime of 400 ps for a "standard" bacteriochlorin as opposed to the observed lifetime of 7 ps for **Benz-BC**.

The reduced excited-state lifetimes caused by β-*meso* annulation of bacteriochlorins does not occur upon addition of the 5-membered isocyclic ring that spans the 13–15 (*meso*–β) positions of native photosynthetic pigments such as bacteriochlorophyll *a*. Unlike the annulated bacteriochlorins studied here, the native 5-membered ring does not provide a conjugation path from *meso* to β-pyrrole positions across the isocyclic unit. Accordingly, the isocyclic ring serves as an auxochrome yet does not impart enhanced internal conversion.

Conclusions

Numerous routes established for annulation of porphyrins were not productive on application to bacteriochlorins. Instead, successive Suzuki–Miyaura coupling enabled construction of the β,*meso*-annulated bacteriochlorins. The photophysical studies of the β,*meso*-annulated bacteriochlorins indicate that this structural motif provides an effective means of bathochromically shifting the lowest energy electronic transition far into the NIR region of the spectrum. The magnitude of the shift is significantly larger than has been achieved *via* addition of typical substituents (*e.g.*, acetyl, formyl, cyano) at the β and/or *meso* positions and also larger than that achieved to date *via* β,β-annulation. A striking photophysical characteristic of the

β,*meso*-annulated bacteriochlorins is an extremely short lowest-excited singlet-state lifetime and accompanying vanishingly small fluorescence quantum yield. The photophysical studies trace these features to extremely rapid internal conversion to the ground electronic state. The origin of the rapid internal conversion is not certain; however, one unusual spectral feature of the two β,*meso*-annulated bacteriochlorins studied herein is exceptionally strong vibronic activity. The strong vibronic activity accompanied by the relatively low energy of the electronic transition possibly open more decay channels to the ground electronic state. The new molecules seem well suited for applications such as photoacoustic imaging[96] or photothermal therapy,[97] where an exquisitely short excited-state lifetime and the absence of fluorescence are desired, but not as NIR fluorescent markers or long-lived energy/electron donors in solar energy conversion.

Experimental section

General methods

^{1}H NMR and ^{13}C NMR spectra were collected at room temperature in $CDCl_3$ unless noted otherwise. Silica (40 μm average particle size) was used for column chromatography. THF was freshly distilled from sodium/benzophenone ketyl. All other solvents (anhydrous or reagent-grade) were employed as received from commercial suppliers. Electrospray ionization mass spectrometry (ESI-MS) data generally enable accurate mass measurements, were obtained in the positive-ion mode (unless noted otherwise), and are reported for the molecular ion or protonated molecular ion. Laser-desorption ionization mass spectrometry without a matrix (LD-MS) or with a matrix (MALDI-MS) affords low resolution data, was carried out in the positive-ion mode with the matrix POPOP, and provided quick screening of reactions. Deactivated silica for purification of acid-labile compounds was prepared by treatment of silica with 5% triethylamine in hexanes (1 g/2 mL) and washing with CH_2Cl_2 followed by hexanes. Commercial compounds were used as received unless noted otherwise. NBS was recrystallized from water. The known compounds **1**,[54] **2**,[68] **8**,[70] **11**,[71] **15**,[45] **20**,[45,73] and **BC-9**[45] were prepared as described in the literature.

Synthesis of bacteriochlorin precursors

***tert*-Butyl 3-formyl-2*H*-dibenzo[*e*,*g*]isoindole-1-carboxylate (3).** Following a reported procedure,[44] DMF (1.0 mL, 13 mmol) was cooled in an ice bath, and $POCl_3$ (1.2 mL, 13 mmol) was added dropwise. An exothermic reaction occurred with the formation of the Vilsmeier complex. The ice bath was removed, and the mixture was stirred at room temperature for 15 min. The mixture was treated with CH_2Cl_2 (6 mL), and the reaction temperature was lowered to 0–2 °C with the aid of a salt-ice bath. A solution of **2** (1.27 g, 4.00 mmol) in CH_2Cl_2 (20 mL) was added to the stirred mixture over a period of 15 min. After the addition was completed, the ice bath was replaced with an oil bath and the mixture was refluxed for 15 min. The mixture was then cooled to 25–30 °C, a solution of sodium acetate (10 g) in water (40 mL) was added dropwise, and the reaction mixture was refluxed for an additional 15 min. The two layers were separated, and the aqueous portion of the mixture was extracted with CH_2Cl_2. The combined organic extract was washed with saturated aqueous Na_2CO_3 solution, dried (Na_2SO_4) and concentrated to afford a pale brown solid (1.14 g, 83%): mp 184–186 °C; ^{1}H NMR δ 1.73 (s, 9H), 7.45–7.62 (m, 4H), 8.16–8.19 (m, 1H), 8.43–8.47 (m, 2H), 9.49–9.53 (m, 1H), 10.32 (s, 1H), 10.35 (s, 1H); ^{13}C NMR δ 28.4, 83.5, 122.7, 123.0, 123.7, 124.2, 125.7, 125.9, 126.30, 126.33, 126.5, 127.1, 127.2, 127.3, 127.4, 127.9, 129.7, 130.8, 159.4, 179.6; ESI-MS obsd 346.1431, calcd 346.1438 [$(M + H)^+$, M = $C_{22}H_{19}NO_3$].

***tert*-Butyl 3-(2-nitroethyl)-2*H*-dibenzo[*e*,*g*]isoindole-1-carboxylate (4).** Following a general procedure,[43] a stirred mixture of **3** (1.04 g, 3.00 mmol), potassium acetate (0.236 g, 2.40 mmol), and methylamine hydrochloride (0.162 g, 2.40 mmol) in absolute ethanol (15 mL) was treated with nitromethane (0.81 mL, 15 mmol). The reaction mixture was heated at 70 °C for 3 h, and then CH_2Cl_2 and water were added. The organic layer was dried (Na_2SO_4) and concentrated. The resulting yellow solid was dried under high vacuum and used directly in the next step. The crude solid material was dissolved in $CHCl_3$/2-propanol (3 : 1, 120 mL). Silica (6 g) and $NaBH_4$ (0.227 g, 6.00 mmol) were added, and the mixture was stirred at room temperature under argon for 30 min. The reaction mixture was filtered, and the filtrate was concentrated. The resulting crude material was dissolved in CH_2Cl_2. The organic solution was washed (water, brine), dried (Na_2SO_4), and concentrated. Column chromatography [silica, hexanes/ethyl acetate (10 : 1)] afforded a white solid (0.562 g, 48%): mp 168–170 °C; ^{1}H NMR (400 MHz) δ 1.73 (s, 9H), 3.79 (t, J = 7.2 Hz, 2H), 4.72 (t, J = 7.2 Hz, 2H), 7.47–7.63 (m, 4H), 7.82–7.85 (m, 1H), 8.49–8.54 (m, 2H), 9.73–9.75 (m, 1H), 9.79 (br s, 1H); ^{13}C NMR (100 MHz) δ 27.1, 28.6, 72.9, 82.1, 115.8, 118.3, 122.4, 122.7, 123.0, 123.9, 124.7, 125.5, 126.9, 127.0, 127.3, 127.4, 127.8, 128.4, 129.5, 130.1, 160.0; ESI-MS obsd 391.1653, calcd 391.1652 [$(M + H)^+$, M = $C_{23}H_{22}N_2O_4$].

***tert*-Butyl 3-(3,3-dimethyl-2-nitro-5-oxohexyl)-2*H*-dibenzo[*e*,*g*]-isoindole-1-carboxylate (5).** Following an established procedure[44] with modification, samples of **4** (156 mg, 0.400 mmol), mesityl oxide (196 mg, 2.00 mmol), TBAF (1.0 M in THF, 0.6 mL, 0.6 mmol), and 4 Å molecular sieves (400 mg) were stirred together in DMF (8 mL) for 4 h. The mixture was then diluted with water (30 mL) and extracted with ethyl acetate (2 × 30 mL). The combined organic extract was washed [HCl solution (2 M, 10 mL), saturated aqueous $NaHCO_3$ solution and brine], dried (Na_2SO_4) and concentrated. The crude solid was triturated with diethyl ether (20 mL) followed by filtration to afford a white solid (0.132 g, 68%): mp 150–152 °C; ^{1}H NMR (400 MHz) δ 1.22 (s, 3H), 1.45 (s, 3H), 1.71 (s, 9H), 2.15 (s, 3H), 2.57 (ABq, $\Delta\delta_{AB}$ = 0.16, J = 18.0 Hz, 2H), 3.71 (d, J = 6.0 Hz, 1H), 3.73 (s, 1H), 5.45–5.49 (m, 1H), 7.51–7.62 (m, 4H), 7.93–7.95 (m, 1H), 8.53–8.59 (m, 2H), 9.67 (br s, 1H), 9.73–9.76 (m, 1H); ^{13}C NMR (100 MHz) δ 23.9, 24.6, 28.0, 28.6, 31.7, 37.2, 51.2, 81.9, 92.5, 116.1, 122.8, 122.96, 123.01, 124.0, 125.5, 126.8, 127.0, 127.1, 127.6, 128.1, 128.5, 129.7, 130.2, 159.9, 206.5; ESI-MS obsd 489.2387, calcd 489.2384 [$(M + H)^+$, M = $C_{29}H_{32}N_2O_5$].

***tert*-Butyl (*Z*)-3-((3,3,5-trimethyl-3,4-dihydro-2*H*-pyrrol-2-ylidene)-methyl)-2*H*-dibenzo[*e*,*g*]isoindole-1-carboxylate (6).** Following a general procedure,[43] in a first flask a solution of **5** (120 mg,

0.246 mmol) in freshly distilled THF (5.0 mL) and anhydrous MeOH (100 μL) at 0 °C was treated with NaOMe (66 mg, 1.2 mmol). The mixture was stirred and degassed by bubbling argon through the solution for 45 min. In a second flask purged with argon, $TiCl_3$ (1.54 mL, 20% w/v in 2 N HCl solution, 2.0 mmol), 8 mL of THF, and NH_4OAc (1.04 g, 13.5 mmol) were combined under argon, and the mixture was degassed by bubbling argon for 45 min. Then the first flask mixture was transferred *via* cannula to the buffered $TiCl_3$ mixture. The resulting mixture was stirred at room temperature for 16 h under argon. Saturated aqueous $NaHCO_3$ was added, and the resulting mixture was then extracted with ethyl acetate. The organic extract was washed with brine, dried (Na_2SO_4), and concentrated. Column chromatography [silica, hexanes/ethyl acetate (10 : 1)] afforded a yellow solid (45 mg, 41%): mp 164–166 °C; ^{1}H NMR δ 1.37 (s, 6H), 1.74 (s, 9H), 2.34 (s, 3H), 2.64 (s, 2H), 6.68 (s, 1H), 7.47–7.66 (m, 4H), 8.40 (d, J = 7.5 Hz, 1H), 8.54–8.60 (m, 2H), 9.93 (dd, J = 8.4 Hz and 1.2 Hz, 1H), 12.82 (br s, 1H); ^{13}C NMR δ 21.0, 28.8, 29.3, 42.0, 54.0, 80.7, 103.1, 116.3, 118.5, 122.9, 123.77, 123.83, 124.9, 126.4, 126.8, 127.0, 127.7, 128.2, 128.5, 129.4, 130.0, 130.2, 160.5, 165.9, 180.8; ESI-MS obsd 439.2376, calcd 439.2380 [(M + H)$^+$, M = $C_{29}H_{30}N_2O_2$].

***tert*-Butyl (*Z*)-3-((5-formyl-3,3-dimethyl-3,4-dihydro-2*H*-pyrrol-2-ylidene)methyl)-2*H*-dibenzo[*e*,*g*]isoindole-1-carboxylate (7).** Following a general procedure,[44] a solution of **6** (45 mg, 0.10 mmol) in 1,4-dioxane (2.0 mL) was treated with SeO_2 (33 mg, 0.30 mmol) under argon. The mixture was stirred for 1.5 h at room temperature. The reaction mixture was treated with saturated aqueous $NaHCO_3$ solution and extracted with ethyl acetate. The organic extract was washed with brine, dried (Na_2SO_4), and concentrated. Column chromatography [silica, hexanes/ethyl acetate (10 : 1)] afforded a dark orange solid (25 mg, 55%): mp 216–218 °C; ^{1}H NMR (400 MHz) δ 1.42 (s, 6H), 1.74 (s, 9H), 2.85 (s, 2H), 7.13 (s, 1H), 7.54–7.67 (m, 4H), 8.36 (d, J = 8.0 Hz, 1H), 8.58–8.62 (m, 2H), 9.85–9.87 (m, 1H), 10.08 (s, 1H), 12.38 (br s, 1H); ^{13}C NMR δ 28.6, 29.3, 41.6, 46.2, 81.6, 112.4, 119.4, 121.2, 122.9, 123.9, 124.0, 124.7, 125.8, 126.2, 126.7, 127.0, 127.2, 127.5, 128.3, 128.4, 130.1, 130.4, 164.3, 171.5, 189.6; ESI-MS obsd 453.2169 calcd 453.2173 [(M + H)$^+$, M = $C_{29}H_{28}N_2O_3$].

4-(Ethoxycarbonyl)-2-formyl-3-(naphthalen-1-yl)pyrrole (9). A solution of **8** (16.9 g, 63.7 mmol) in DMF (300 mL) was treated with $POCl_3$ (7.1 mL, 76 mmol) at 0 °C. The resulting mixture was stirred under argon at 0 °C for 1 h, and then 16 h at room temperature. The reaction mixture was treated with a mixture of saturated aqueous sodium acetate/CH_2Cl_2 [400 mL, 3 : 1 (v/v)] and stirred for 1 h. The water phase was separated and extracted with CH_2Cl_2. The combined organic phase was washed with a saturated LiCl solution, dried (Na_2SO_4) and concentrated. The resulting solid was chromatographed [silica, hexanes/ethyl acetate (2 : 1)] to give a light-brown solid (12.9 g, 69%): mp 147–150 °C; ^{1}H NMR (300 MHz, $CDCl_3$) δ 0.73 (t, J = 7.2 Hz, 3H), 3.82–4.04 (m, 2H), 7.32–7.58 (m, 4H), 7.65 (d, J = 7.4 Hz, 1H), 7.80 (s, 1H), 7.90 (t, J = 6.9 Hz, 2H), 9.18 (d, J = 1.1 Hz, 1H), 11.10 (br s, 1H); ^{13}C NMR (75 MHz, $CDCl_3$) δ 13.7, 60.2, 118.7, 125.1, 126.1, 126.3, 126.5, 128.4, 128.7, 128.9, 129.9, 130.9, 131.7, 133.5, 135.9, 163.8, 181.1; anal. calcd for $C_{18}H_{15}NO_3$: C, 73.71; H, 5.15; N, 4.78. Found: C, 73.41; H, 4.99; N, 4.81. ESI-MS obsd 316.0937, calcd 316.0944 [(M + Na)$^+$, M = $C_{18}H_{15}NO_3$].

4-(Ethoxycarbonyl)-3-(naphthalen-1-yl)-2-(2-nitroethyl)pyrrole (10). Following a general procedure,[43] a stirred mixture of **9** (12.6 g, 43.0 mmol), potassium acetate (3.3 g, 34 mmol), and methylamine hydrochloride (2.3 g, 34 mmol) in absolute ethanol (16 mL) was treated with nitromethane (6.0 mL, 0.11 mol). The mixture was stirred for 2 h, whereupon water was added. The reaction mixture was filtered, and the filtered material was washed with water and a small amount of cold water/ethanol (1 : 1). The filtered material was dried under high vacuum to afford a yellow solid, which was used directly in the next step. The crude solid material was dissolved in $CHCl_3$/2-propanol (3 : 1, 390 mL). Silica (34 g) and $NaBH_4$ (3.0 g, 78 mmol) were added, and the mixture was stirred at room temperature under argon for 2 h. The reaction mixture was filtered, and the filtrate was washed with saturated aqueous $NaHCO_3$. The organic layer was separated and concentrated to afford a pale brown solid (10 g, 69%): mp 48–52 °C; ^{1}H NMR (300 MHz, $CDCl_3$) δ 0.73 (t, J = 7.0 Hz, 3H), 2.98 (dt, J = 17.6, 6.5 Hz, 2H), 3.88 (dq, J = 18.7, 3.6 Hz, 2H), 4.20 (t, J = 6.5 Hz, 2H), 7.28–7.60 (m, 5H), 7.85 (t, J = 7.8 Hz, 3H), 8.96 (br s, 1H); ^{13}C NMR (75 MHz, $CDCl_3$) δ 13.8, 23.7, 59.6, 75.0, 116.8, 122.0, 124.2, 125.5, 125.9, 126.0, 126.1, 126.2, 127.88, 127.91, 128.4, 132.9, 133.7, 164.9; anal. calcd for $C_{19}H_{18}N_2O_4$: C, 67.44; H, 5.36; N, 8.28. Found: C, 66.95; H, 5.27; N, 7.86. ESI-MS obsd 361.1267, calcd 361.1154 [(M + Na)$^+$, M = $C_{19}H_{18}N_2O_4$].

6-(4-(Ethoxycarbonyl)-3-(naphthalen-1-yl)pyrrol-2-yl)-1,1-dimethoxy-4,4-dimethyl-5-nitrohexan-2-one (12). Following a general procedure,[43] a mixture of **10** (9.3 g, 28 mmol) and **11** (8.8 g, 55 mmol) was treated with DBU (12.3 mL, 82.5 mmol). The reaction mixture was stirred at room temperature for 16 h under argon. A saturated solution of cold aqueous NH_4Cl was added. The mixture was extracted with ethyl acetate, and the organic layer was washed with brine, dried (Na_2SO_4), and concentrated. Column chromatography [silica, CH_2Cl_2/ethyl acetate (9 : 1)] afforded an amorphous brown solid (7.9 g, 47%): ESI-MS obsd 497.2277, calcd 497.2282 [(M + H)$^+$, M = $C_{27}H_{32}N_2O_7$]; NMR data were collected from pure fractions of the two existing rotamers. Rotamer A: ^{1}H NMR (300 MHz, $CDCl_3$) δ 0.78 (s, 3H), 0.82 (s, 3H), 1.24 (t, J = 7.2 Hz, 3H), 2.28, 2.45 (AB, ^2J = 18.2 Hz, 2H), 2.56 (ABX, $^3J_{BX}$ = 2.2 Hz, $^2J_{AB}$ = 15.1 Hz, 1H), 3.05 (ABX, $^3J_{AX}$ = 11.6 Hz, $^2J_{AB}$ = 15.1 Hz, 1H), 3.28 (s, 3H) 3.32 (s, 3H), 3.82–4.01 (m, 2H), 4.22 (s, 1H), 4.92 (ABX, $^3J_{BX}$ = 2.2 Hz, $^3J_{AX}$ = 11.6 Hz, 1H), 7.30–7.65 (m, 5H), 7.75–7.91 (m, 3H), 9.29 (br s, 1H); ^{13}C NMR (75 MHz, $CDCl_3$) δ 13.9, 23.6, 23.9, 25.5, 36.4, 44.7, 55.0, 55.1, 59.5, 77.1, 95.1, 104.4, 116.3, 121.8, 124.4, 125.5, 125.8, 126.1, 126.4, 127.7, 128.3, 128.5, 133.0, 133.5, 133.7, 165.1, 203.4. Rotamer B: ^{1}H NMR (300 MHz, $CDCl_3$) δ 0.74 (s, 3H), 0.76 (s, 3H), 1.24 (t, J = 7.2 Hz, 3H), 2.20, 2.43 (AB, ^2J = 18.2 Hz, 2H), 2.80 (ABX, $^3J_{BX}$ = 2.2 Hz, $^2J_{AB}$ = 15.1 Hz, 1H), 2.99 (ABX, $^3J_{AX}$ = 11.6 Hz, $^2J_{AB}$ = 15.1 Hz, 1H), 3.29 (s, 3H), 3.30 (s, 3H), 3.77–4.04 (m, 2H), 4.16 (s, 1H), 4.55 (ABX, $^3J_{BX}$ = 2.2 Hz, $^3J_{AX}$ = 11.6 Hz, 1H), 7.28–7.67 (m, 5H), 7.77–7.90 (m, 3H), 9.34 (br s, 1H); ^{13}C NMR (75 MHz, $CDCl_3$) δ 13.8, 23.5, 23.7, 25.3, 36.4, 44.2, 55.07, 55.14, 59.6, 77.0, 94.8, 104.4, 116.5, 121.9,

124.4, 125.4, 125.8, 126.1, 126.4, 127.70, 127.71, 128.2, 133.1, 133.7, 133.9, 165.1, 203.3.

8-(Ethoxycarbonyl)-2,3-dihydro-1-(1,1-dimethoxymethyl)-7-(naphthalen-1-yl)-3,3-dimethyldipyrrin (13). Following a general procedure,[43] in a first flask, a solution of **12** (6.65 g, 13.4 mmol) in freshly distilled THF (30 mL) and anhydrous MeOH (1.0 mL) at 0 °C was treated with NaOMe (2.2 g, 40 mmol). The mixture was stirred and degassed by bubbling argon through the solution for 45 min. In a second flask purged with argon, $TiCl_3$ (50 mL, 20% wt/v in 3% HCl solution, 80 mmol), 125 mL THF, NH_4OAc (50 g, 650 mmol) and water (20 mL) were combined under argon, and the mixture was degassed by bubbling argon for 45 min. Then, the first flask mixture was transferred *via* cannula to the buffered $TiCl_3$ mixture. The resulting mixture was stirred at room temperature for 16 h under argon. The reaction mixture was then poured over a pad of Celite and eluted with ethyl acetate. The eluant was washed with a saturated aqueous solution of $NaHCO_3$. The organic layer was dried (Na_2SO_4) and concentrated. Column chromatography [silica, CH_2Cl_2/ethyl acetate (98 : 2)] afforded an amorphous brown solid (3.34 g, 56%): ^{1}H NMR (400 MHz, $CDCl_3$) δ 0.65 (t, J = 7.2 Hz, 3H), 0.98 (s, 3H), 1.08 (s, 3H), 2.59 (s, 2H), 3.48 (s, 6H), 3.75–3.96 (m, 2H), 5.07 (s, 1H), 5.52 (s, 1H), 7.30–7.47 (m, 3H), 7.48–7.55 (m, 1H), 7.67 (d, J = 2.9 Hz, 1H), 7.70–7.76 (m, 1H), 7.81–7.90 (m, 2 H), 11.31 (br s, 1H); ^{13}C NMR (100 MHz, $CDCl_3$) δ 13.7, 29.1, 29.2, 40.5, 48.6, 54.9, 59.4, 102.8, 105.6, 116.6, 125.3, 125.5, 125.6, 127.1, 127.4, 128.1, 128.5, 130.5, 133.4, 133.7, 134.1, 161.6, 165.2, 175.7; ESI-MS obsd 447.2258, calcd 447.2278 [$(M + H)^+$, M = $C_{27}H_{30}N_2O_4$].

4-(Ethoxycarbonyl)-2-iodo-3-(naphthalen-1-yl)pyrrole (14). Following a literature procedure[45] with slight modification, a stirred solution of **15** (3.98 g, 15.0 mmol) in anhydrous DMF (75.0 mL) was treated with NIS (3.38 g, 15.0 mmol) in batches at 0 °C. After 2 h, the reaction mixture was diluted with ethyl acetate (150 mL) and washed with water and brine. The organic layer was dried (Na_2SO_4) and filtered. The filtrate was concentrated and chromatographed [silica, hexanes/ethyl acetate (4 : 1)] to give a pale yellow crystalline solid (2.85 g, 48%): mp 199–200 °C; ^{1}H NMR (400 MHz, $CDCl_3$) δ 0.67 (t, J = 7.6 Hz, 3H), 3.80–3.98 (m, 2H), 7.32–7.40 (m, 2H), 7.42–7.48 (m, 1H), 7.48–7.54 (m, 1H), 7.57 (d, J = 8.4 Hz, 1H), 7.65 (d, J = 2.8 Hz, 1H), 7.82–7.94 (m, 2H), 8.78 (br s, 1H); ^{13}C NMR (100 MHz, $CDCl_3$) δ 13.3, 59.6, 117.2, 125.1, 125.4, 125.5, 126.2, 127.6, 128.0, 128.1, 128.2, 128.4, 129.1, 133.1, 133.3, 133.7, 164.1; ESI-MS obsd 392.0143, calcd 392.0142 [$(M + H)^+$, M = $C_{17}H_{14}INO_2$].

4-(Ethoxycarbonyl)-(*E*)-2-(1-(4,4-dimethyl-5-oxodihydrofuran-2(3*H*)-ylidene)methyl)-3-(naphthalen-1-yl)pyrrole (16). Following a literature procedure[45] with slight modification, a mixture of **14** (2.4 g, 6.1 mmol), **15** (1.55 g, 12.3 mmol), and $BnNEt_3Cl$ (1.4 g, 6.1 mmol) in anhydrous acetonitrile (25.0 mL) and triethylamine (6.1 mL) in a Schlenk flask was deaerated by three freeze–pump–thaw cycles. Then, a sample of $Pd(PPh_3)_4$ (354 mg, 0.307 mol, 5 mol%) was added, and the resulting reaction mixture was further deaerated. The reaction mixture was stirred and heated at 80 °C for 24 h. After allowing to cool to room temperature, CH_2Cl_2 and water were added. The organic layer was separated, dried (Na_2SO_4) and filtered. The filtrate was concentrated and chromatographed [silica, hexanes/ethyl acetate (3 : 1)] to afford a pale yellow crystalline solid (1.83 g, 76%): mp 202–203 °C; ^{1}H NMR (400 MHz, $CDCl_3$) δ 0.69 (t, J = 7.2 Hz, 3H), 1.07 (s, 3H), 1.14 (s, 3H), 2.50 (dd, J = 2.0, 16.0 Hz, 1H), 2.40 (dd, J = 2.0, 16.0 Hz, 1H), 3.78–3.98 (m, 2H), 5.93 (dd, J = 2.0, 2.0 Hz, 1H), 7.30–7.40 (m, 2H), 7.40–7.52 (m, 2H), 7.60 (d, J = 3.2 Hz, 1H), 7.63–7.67 (m, 1H), 7.79–7.87 (m, 2H), 8.50 (br s, 1H); ^{13}C NMR (100 MHz, $CDCl_3$) δ 13.6, 24.6, 24.9, 39.6, 39.9, 59.5, 97.5, 116.5, 122.2, 125.07, 125.14, 125.5, 125.6, 126.2, 127.5, 128.17, 128.21, 132.8, 133.3, 133.5, 147.6, 165.0, 179.6; ESI-MS obsd 390.1701, calcd 390.1700 [$(M + H)^+$, M = $C_{24}H_{23}NO_4$].

4-(Ethoxycarbonyl)-(*E*)-2-(1-(4,4-dimethyl-5-methylenedihydrofuran-2(3*H*)-ylidene)methyl)-3-(naphthalen-1-yl)pyrrole (17). Following a standard procedure,[45] a solution of $TiCp_2Cl_2$ (3.045 g, 12.37 mmol) in toluene (33 mL) was treated dropwise with MeLi solution (17 mL in Et_2O, 27 mmol, 1.6 M) at 0 °C under an argon atmosphere. After 1 h at 0 °C, saturated aqueous NH_4Cl solution was added. The organic layer was washed with water and brine, dried (Na_2SO_4), and filtered. The filtrate (now ~30–40 mL owing to solvent losses in handling) contained the Petasis reagent. The filtrate in its entirety was treated with **16** (1.02 g, 2.61 mmol) and additional $TiCp_2Cl_2$ (39 mg). The solution was heated to 80 °C in the dark for 6 h under argon. Afterward, the resulting mixture was allowed to cool to room temperature whereupon MeOH (3.1 mL), $NaHCO_3$ (130 mg), and water (31 μL) were added. The mixture was kept at 40 °C for 12 h with stirring and then filtered through Celite. The filtrate was concentrated under reduced pressure. Column chromatography [silica, hexanes/ethyl acetate (3 : 1)] afforded a yellow crystalline solid (733 mg, 72%): mp 158–159 °C; ^{1}H NMR (400 MHz, $CDCl_3$) δ 0.68 (t, J = 7.2 Hz, 3H), 1.07 (s, 3H), 1.13 (s, 3H), 2.26–2.50 (m, 2H), 3.76–3.98 (m, 3H), 4.24 (d, J = 2.4 Hz, 1H), 5.64 (s, 1H), 7.28–7.38 (m, 2H), 7.38–7.50 (m, 2H), 7.54 (d, J = 3.6 Hz, 1H), 7.67 (d, J = 8.4 Hz, 1H), 7.74–7.84 (m, 2H), 8.45 (br s, 1H); ^{13}C NMR (100 MHz, $CDCl_3$) δ 13.6, 27.3, 27.7, 40.2, 41.8, 59.4, 80.3, 92.3, 116.6, 120.6, 124.0, 125.2, 125.3, 125.4, 126.4, 127.2, 127.4, 128.0, 128.3, 133.3, 133.51, 133.54, 153.3, 165.1, 168.9; ESI-MS obsd 388.1913, calcd 388.1907 ([$(M + H)^+$, M = $C_{25}H_{25}NO_3$).

8-(Ethoxycarbonyl)-1-methyl-2,2-dimethyl-7-(naphthalen-1-yl)-2,3-dihydrodipyrrin (18). Following a literature procedure[45] with slight modification, a solution of **17** (660 mg, 1.7 mmol) in DMF (17 mL) was treated with 1 M HCl (1.0 mL). After 30 min, NH_4OAc (2.63 g, 34.1 mmol) and triethylamine (4.8 mL, 35 mmol) were added. The resulting mixture was stirred at 55 °C for 16 h. The reaction was quenched by the addition of saturated aqueous KH_2PO_4 solution. The resulting mixture was extracted with ethyl acetate (100 mL). The organic layer was washed with water, dried (Na_2SO_4), and filtered. The filtrate was concentrated and chromatographed [silica, hexanes/ethyl acetate (3 : 1)] to afford a light-yellow crystalline solid (520 mg, 79%): mp 73–75 °C; ^{1}H NMR (400 MHz, $CDCl_3$) δ 0.65 (t, J = 7.2 Hz, 3H), 1.12 (s, 3H), 1.14 (s, 3H), 2.15 (s, 3H), 2.39 (q, J = 16.8 Hz, 2H), 3.74–3.96 (m, 2H), 5.47 (s, 1H), 7.30–7.46 (m, 3H), 7.50 (t, J = 7.6 Hz, 1H), 7.64 (d, J = 3.2 Hz, 1H), 7.71 (d, J = 8.4 Hz, 1H), 7.82 (d, J = 8.0 Hz, 1H), 7.85

(d, J = 8.0 Hz, 1H), 11.44 (br s, 1H); ^{13}C NMR (100 MHz, $CDCl_3$) δ 13.5, 15.7, 25.6, 25.7, 43.9, 48.4, 59.1, 104.2, 116.2, 120.7, 124.5, 125.1, 125.3, 125.4, 126.9, 127.1, 127.9, 128.3, 130.8, 133.4, 133.6, 134.0, 150.5, 165.1, 187.5; ESI-MS obsd 387.2076, calcd 387.2067 [$(M + H)^+$, M = $C_{25}H_{26}N_2O_2$].

8-(Ethoxycarbonyl)-1-(1,1-dimethoxymethyl)-2,2-dimethyl-7-(naphthalen-1-yl)-2,3-dihydrodipyrrin (19). Following a literature procedure[45] with slight modification, a solution of **18** (193 mg, 0.499 mmol) in 1,4-dioxane (9 mL) was treated with SeO_2 (166 mg, 1.50 mmol) at room temperature. After 30 min, ethyl acetate and water were added. The organic layer was washed with brine, dried (Na_2SO_4), and concentrated under reduced pressure. The residue was dissolved in $HC(OMe)_3$ (4.0 mL) and treated with p-TsOH·H_2O (29 mg, 0.15 mmol) at room temperature. After 12 h, the reaction mixture was quenched by the addition of saturated aqueous $NaHCO_3$ solution and then extracted with ethyl acetate. The organic layer was dried (Na_2SO_4) and filtered. The filtrate was concentrated and chromatographed [silica, hexanes/ethyl acetate (4 : 1)] to afford a brown viscous liquid (93 mg, 42%): ^{1}H NMR (400 MHz, $CDCl_3$) δ 0.66 (t, J = 7.6 Hz, 3H), 1.20 (s, 3H), 1.23 (s, 3H), 2.30–2.54 (m, 2H), 3.46 (s, 3H), 3.47 (s, 3H), 3.70–4.00 (m, 2H), 5.13 (s, 1H), 5.62 (t, J = 2.0 Hz, 1H), 7.30–7.60 (m, 4H), 7.60–7.80 (m, 2H), 7.80–8.00 (m, 2H), 11.27 (br s, 1H); ^{13}C NMR (100 MHz, $CDCl_3$) δ 13.5, 25.9, 26.0, 45.6, 48.2, 54.46, 54.48, 59.1, 102.0, 107.4, 116.3, 121.8, 125.1, 125.2, 125.4, 125.5, 126.8, 127.2, 128.0, 128.3, 130.4, 133.3, 133.4, 133.9, 149.5, 165.0, 182.0; ESI-MS obsd 447.2288, calcd 447.2278 [$(M + H)^+$, M = $C_{27}H_{30}N_2O_4$].

3-Bromo-4-ethoxycarbonyl-(*E*)-2-[(4,4-dimethyl-5-oxodihydrofuran-2(3*H*)-ylidene)methyl]pyrrole (21). A suspension of K_2CO_3 (497.6 mg, 3.600 mmol) in MeCN was treated with 2,4,6-tribromophenol (661.6 mg, 2.000 mmol) at room temperature. After 30 min, the mixture was cooled to 0 °C. Compound **20** (263.3 mg, 1.000 mmol) followed by 2,4,4,6-tetrabromo-2,5-cyclohexadienone (655.5 mg, 1.600 mmol) were added at 0 °C. After 1 h at 0 °C, the reaction mixture was diluted with ethyl acetate (10 mL). The mixture was washed with aqueous $NaHSO_3$ (10%, 10 mL), saturated aqueous $NaHCO_3$ (10 mL), and brine (10 mL). The organic layer was dried (Na_2SO_4) and concentrated under reduced pressure. Column chromatography [silica, hexanes/ethyl acetate (7 : 3)] afforded a pale orange solid (210.3 mg, 61%): mp 81 °C (dec.); ^{1}H NMR (400 MHz, $CDCl_3$) δ 1.35 (s, 6H), 1.36 (t, J = 7.2 Hz, 3H), 2.91 (d, J = 2.0 Hz, 2H), 4.31 (q, J = 7.2 Hz, 2H), 6.21 (t, J = 2.0 Hz, 1H), 7.46 (d, J = 3.2 Hz, 1H), 8.59 (br s, 1H); ^{13}C NMR (100 MHz, $CDCl_3$) δ 14.4, 25.1, 40.3, 60.3, 96.7, 97.8, 115.2, 125.4, 126.1, 149.7, 163.8, 179.7; ESI-MS obsd 342.0328, calcd 342.0336 [$(M + H)^+$, M = $C_{14}H_{16}BrNO_4$].

5-Bromo-4-ethoxycarbonyl-(*E*)-2-[(4,4-dimethyl-5-oxodihydrofuran-2(3*H*)-ylidene)methyl]pyrrole (22). A solution of **20** (39.5 mg, 0.150 mmol) in DMF (1.50 mL) at −20 °C was treated with NBS (26.7 mg, 0.150 mmol). After 30 min, the reaction mixture was allowed to warm to room temperature. After 9.5 h, saturated aqueous $Na_2S_2O_4$ (1 mL) and ethyl acetate (1 mL) was added. The mixture was washed with H_2O (5 mL) and brine (2 mL). The organic layer was dried (Na_2SO_4) and chromatographed [silica, hexanes/ethyl acetate (4 : 1)] to afford the title compound (25.9 mg, 50%) as a white solid and **21** (9.2 mg, 18%) as a white solid. Data for the title compound: mp 75 °C (dec.); ^{1}H NMR (400 MHz, $CDCl_3$) δ 1.37 (s, 6H), 1.38 (t, J = 7.2 Hz, 3H), 2.94 (d, J = 1.8 Hz, 2H), 4.33 (q, J = 7.2 Hz, 2H), 6.10 (t, J = 1.8 Hz, 1H), 6.40 (d, J = 2.4 Hz, 1H), 8.74 (br s, 1H); ^{13}C NMR (100 MHz, $CDCl_3$) δ 14.6, 25.5, 40.1, 40.7, 60.5, 96.9, 104.8, 109.0, 116.1, 128.0, 149.0, 163.6, 179.7; ESI-MS obsd 342.0327, calcd 342.0336 [$(M + H)^+$, M = $C_{14}H_{16}BrNO_4$].

7-Bromo-8-ethoxycarbonyl-1,2,2-trimethyl-2,3-dihydrodipyrrin (23). Following a reported procedure[45] with modification, MeLi (6.52 mL, 10.4 mmol, 1.6 M in Et_2O) was added dropwise to a solution of $TiCp_2Cl_2$ (1.180 g, 4.740 mmol) in toluene (12.6 mL) at 0 °C. After 1 h at 0 °C, the reaction mixture was washed with aqueous NH_4Cl (6%, 11 mL), H_2O (11 mL), and brine (11 mL). The organic layer was dried (Na_2SO_4) and filtered. Samples of **21** (342.2 mg, 1.000 mmol) and additional $TiCp_2Cl_2$ (14.9 mg, 0.0598 mmol) were added to the filtrate containing the Petasis reagent at room temperature. The mixture was heated to 80 °C in the dark for 2.5 h and then allowed to cool to room temperature. $NaHCO_3$ (50 mg), MeOH (1.2 mL), and H_2O (12 μL, 0.1% v/v relative to MeOH) were added. The mixture was heated to 40 °C for 14 h and filtered through Celite. The filtrate was concentrated under reduced pressure. DMF (9.6 mL) and aqueous HCl (6 M, 84 μL, 0.50 mmol) were added to the residue at room temperature. Aqueous HCl (6 M, 3 × 84 μL, 3 × 0.50 mmol) was added after 100, 110, and 240 min. After 3 h at room temperature, NH_4OAc (1.574 g, 20.42 mmol) and NEt_3 (2.84 mL, 20.4 mmol) were added. After 12 h at room temperature, the reaction mixture was quenched with aqueous KH_2PO_4 (10%, 10 mL) and extracted with CH_2Cl_2 (10 mL). The organic layer was washed with H_2O (40 mL) and brine (40 mL). The organic layer was dried (Na_2SO_4) and filtered. The filtrate was concentrated under reduced pressure. Column chromatography [silica, hexanes/ethyl acetate (4 : 1)] afforded a yellow solid (219.0 mg, 65%): ^{1}H NMR (300 MHz, $CDCl_3$) δ 1.37 (s, 6H), 1.36 (t, J = 7.1 Hz, 3H), 2.14 (s, 3H), 2.60 (d, J = 1.8 Hz, 2H), 4.30 (q, J = 7.1 Hz, 2H), 5.98 (s, 1H), 7.45 (d, J = 2.7 Hz, 1H), 11.40 (br s, 1H); ^{13}C NMR (75 MHz, $CDCl_3$) δ 14.6, 15.9, 25.6, 44.2, 48.6, 59.9, 95.5, 103.2, 114.4, 124.6, 131.1, 151.9, 163.9, 188.7; ESI-MS obsd 339.0703, calcd 339.0703 [$(M + H)^+$, M = $C_{15}H_{19}BrN_2O_2$].

Bis(7-bromo-8-carbethoxy-2,3-dihydro-1,2,2-trimethyldipyrrinato)palladium(II) (24). Following a reported method[75] with some modification, a solution of **23** (15 mg, 43 μmol) in CH_2Cl_2 (0.50 mL) was treated with $Pd(OAc)_2$ (19 mg, 86 μmol). The reaction mixture was stirred at r.t. for 2 h and then chromatographed [silica, hexanes/ethyl acetate (2 : 1 to 1 : 1)] to afford a yellow-green solid (6.0 mg, 36%): mp >230 °C (dec.); ^{1}H NMR ($CDCl_3$, 400 MHz) δ 6.80 (s, 2H), 6.32 (s, 2H), 4.30–4.15 (m, 4H), 2.85 (d, J = 14.8 Hz, 2H), 2.65 (d, J = 14.8 Hz, 2H), 1.71 (s, 6H), 1.30–1.26 (m, 12H), 1.04 (s, 6H); ^{13}C NMR ($CDCl_3$, 100 MHz) δ 195.6, 163.6, 139.4, 136.2, 131.7, 115.5, 110.5, 97.3, 59.1, 49.5, 43.8, 25.5, 23.3, 17.0, 14.6; ESI-MS obsd 781.0204, calcd 781.0211 [$(M + H)^+$, M = $C_{30}H_{36}Br_2N_2O_4Pd$]; λ_{abs} (toluene) 364 nm.

7-Bromo-8-ethoxycarbonyl-1-(1,1-dimethoxymethyl)-2,2-dimethyl-2,3-dihydrodipyrrin (25). Following a literature procedure[45] with

slight modification, a solution of **23** (111.9 mg, 0.3299 mmol) and pyridine (53 μL) in 1,4-dioxane (6.60 mL) was treated with SeO_2 (73.2 mg, 0.660 mmol) at room temperature. After 5 h, the reaction mixture was diluted with ethyl acetate (10 mL) and filtered through Celite. The filtrate was washed with H_2O (10 mL) and brine (10 mL). The organic layer was dried (Na_2SO_4), filtered, and concentrated under reduced pressure. The residue was treated with trimethyl orthoformate (3.30 mL) and *p*-TsOH·H_2O (12.6 mg, 0.066 mmol) at room temperature. After 1.5 h, the reaction mixture was quenched with saturated aqueous $NaHCO_3$ (5 mL) and extracted with ethyl acetate (5 mL). The organic layer was washed with brine (5 mL), dried (Na_2SO_4), and filtered. The filtrate was concentrated and twice chromatographed [silica, hexanes/ethyl acetate (4 : 1) for the first chromatography, CH_2Cl_2/ethyl acetate (20 : 1) for the second chromatography] to afford a pale orange solid (48.3 mg, 37%): ^{1}H NMR (300 MHz, $CDCl_3$) δ 1.29 (s, 6H), 1.35 (t, J = 7.2 Hz, 3H), 2.63 (d, J = 1.8 Hz, 2H), 3.45 (s, 6H), 4.30 (q, J = 7.2 Hz, 2H), 5.11 (s, 1H), 6.13 (t, J = 1.8 Hz, 1H), 7.48 (d, J = 3.6 Hz, 1H), 11.19 (br s, 1H); ^{13}C NMR (100 MHz, $CDCl_3$) δ 14.5, 26.0, 45.8, 48.5, 54.5, 59.9, 96.8, 101.9, 106.4, 114.6, 125.3, 130.7, 150.9, 163.8, 183.1; ESI-MS obsd 399.0907, calcd 399.0914 [$(M + H)^+$, M = $C_{17}H_{23}BrN_2O_4$].

(8-Bromonaphthalen-1-yl)boronic acid (26)[82,83]. A solution of 1,8-dibromonaphthalene (1.430 g, 5.00 mmol) in THF at −60 °C was treated dropwise with *n*-butyllithium (3.34 mL, 1.6 M in hexane) over 5 min. After 1 h at −60 °C, trimethyl borate (668 μL, 6.00 mmol) was added dropwise at −60 °C. Then, the reaction mixture was allowed to warm to room temperature. After 2.5 h, saturated aqueous NH_4Cl (50 mL) was added at room temperature. After 2.5 h, the mixture was extracted with ethyl acetate (50 mL). The organic layer was washed with brine (50 mL), dried (Na_2SO_4), and filtered. The filtrate was concentrated and chromatographed [silica, hexanes/acetone (7 : 3)] to afford a white solid (823.9 mg, 59%): ^{1}H NMR (400 MHz, acetone-d_6) δ 7.20 (s, 2H), 7.38 (dd, J = 8.0, 7.6 Hz, 1H), 7.52 (dd, J = 8.0, 6.8 Hz, 1H), 7.63 (dd, J = 6.8, 1.2 Hz, 1H), 7.83 (dd, J = 7.6, 1.2 Hz, 1H), 7.90 (dd, J = 8.0, 1.2 Hz, 1H), 7.93 (dd, J = 8.0, 1.2 Hz, 1H); ^{13}C NMR (125 MHz, acetone-d_6) δ 124.2, 126.75, 126.83, 129.5, 129.6, 131.3, 132.4, 134.5, 136.0; ESI-MS obsd 272.6963, calcd 272.6963 [$(M + Na)^+$, M = $C_{10}H_9BBrO_2$].

Synthesis of bacteriochlorins

2,3,12,13-Tetrabromo-8,8,18,18-tetramethylbacteriochlorin (BC-1). Following a standard procedure,[42] a solution of **1** (348 mg, 0.857 mmol, 18 mM) in anhydrous CH_3CN (48 mL) was treated with BF_3·OEt_2 (0.83 mL, 6.7 mmol, 140 mM). The reaction mixture was stirred at room temperature for 15 h. Excess triethylamine (2.0 mL) was added to the reaction mixture. The reaction mixture was concentrated, and the residue was chromatographed [silica, hexanes/CH_2Cl_2 (19 : 1)] to afford a green solid (46 mg, 16%): ^{1}H NMR (400 MHz, $CDCl_3$) δ −1.86 (br s, 2H), 1.96 (s, 12H), 4.43 (s, 4H), 8.75 (s, 2H), 8.88 (s, 2H); ^{13}C NMR (150 MHz, $CDCl_3$) δ 30.97, 46.18, 51.38, 95.64, 97.85, 113.4, 113.5, 132.0, 132.9, 159.9, 171.9; ESI-MS obsd 681.8571, calcd 681.8573 [$(M)^+$, M = $C_{24}H_{22}Br_4N_4$]; λ_{abs} (CH_2Cl_2) 347, 373, 496, 743 nm.

2,3,12,13-Tetrakis(methoxycarbonylvinyl)-8,8,18,18-tetramethylbacteriochlorin (BC-2). Following a reported procedure[59] with slight modification, bacteriochlorin **BC-1** (12.0 mg, 17.5 μmol), $Pd(OAc)_2$ (11.9 mg, 53.0 μmol), PPh_3 (32.8 mg, 0.125 mmol) and K_2CO_3 (21.0 mg, 0.152 mmol) were added to a Schlenk tube and dried under high vacuum. The vacuum was released under argon to allow the addition of a solution of DMF (3 mL), toluene (3 mL) and methyl acrylate (175 μL, 1.93 mmol). The mixture was then deaerated *via* four freeze–pump–thaw cycles before the vessel was purged again with argon. The Schlenk flask was sealed and heated at 105 °C for 10 h. The resulting mixture was washed with water (20 mL) and extracted with CH_2Cl_2 (2 × 20 mL). The combined organic extract was dried (Na_2SO_4) and concentrated. The residue was first purified by chromatography [deactivated silica, hexanes/CH_2Cl_2 (2 : 1 to 1 : 1)], then on preparative TLC to afford a reddish solid (4.0 mg, 32%): ^{1}H NMR (600 MHz, $CDCl_3$) δ −0.93 (s, 2H), 1.94 (s, 12H), 4.01 (s, 6H), 4.02 (s, 6H), 4.37 (s, 4H), 6.92 (d, J = 16.0 Hz, 4H), 8.69 (s, 2H), 8.83 (s, 2H), 8.97 (t, J = 16.4 Hz, 4H); ^{13}C NMR (150 MHz, $CDCl_3$) δ 30.8, 46.2, 51.7, 52.1, 52.1, 95.1, 97.4, 124.5, 124.6, 126.8, 126.9, 134.0, 134.9, 137.1, 137.2, 161.3, 167.2, 167.3, 173.2; ESI-MS obsd 706.2990, calcd 706.2997 [M^+, M = $C_{40}H_{42}N_4O_8$]; λ_{abs} (CH_2Cl_2) 319, 359, 393, 543, 815 nm.

BC-3. Following an established procedure,[44] a sample of **7** (21 mg, 0.046 mmol) was dissolved in TFA (2.6 mL) under argon and stirred for 2 h at room temperature. Then the reaction mixture was poured into saturated aqueous $NaHCO_3$ solution and extracted with CH_2Cl_2. The organic extract was washed with brine and water, dried (Na_2SO_4), and concentrated. The residue was washed with Et_2O followed by MeOH. The title compound could not be fully characterized because of instability; with only limited data obtained the assignment remains provisional: LD-MS obsd 670.8 [M^+, M = $C_{28}H_{38}N_4$]; λ_{abs} (CH_2Cl_2) 801 nm; λ_{flu} (CH_2Cl_2) 808 nm.

3,13-Bis(ethoxycarbonyl)-2,12-di(naphthalen-1-yl)-8,8,18,18-tetramethylbacteriochlorin (BC-4). Following an established procedure,[42] a solution of **13** (2.31 g, 5.17 mmol, 18 mM) in anhydrous CH_3CN (290 mL) was treated with BF_3·OEt_2 (5.1 mL, 41 mmol, 140 mM). The reaction mixture was stirred at room temperature for 16 h. The reaction was quenched by the addition of solid $NaHCO_3$ to the reaction mixture. The mixture was filtered. The filtrate was concentrated, and the residue was chromatographed [silica, CH_2Cl_2/hexanes (2 : 1)] to afford a purple/green solid (825 mg, 41%). The ^{1}H NMR spectrum indicated a mixture of atropisomers (~1 : 1 ratio): ^{1}H NMR (500 MHz, $CDCl_3$) δ −0.98 (br s, 4H), 0.66 (t, J = 7.0 Hz, 12H), 1.67 (m, 12H), 1.86 (m, 12H), 4.12–4.19 (m, 8H), 4.34–4.43 (m, 8H), 7.30 (t, J = 7.5 Hz, 4H), 7.54 (t, J = 7.5 Hz, 4H), 7.68 (d, J = 8.5 Hz, 4H), 7.81 (t, J = 7.5 Hz, 4H), 7.93 (d, J = 7.0 Hz, 4H), 8.07 (d, J = 8.0 Hz, 4H), 8.15 (d, J = 8.0 Hz, 4H), 8.37 (s, 4H), 9.86 (s, 4H); ^{13}C NMR (100 MHz, $CDCl_3$) δ 13.5, 30.8, 30.95, 31.04, 46.1, 52.1, 60.7, 97.7, 99.4, 125.3, 126.1, 126.3, 127.0, 128.4, 128.6, 130.0, 133.8, 134.1, 134.6, 135.0, 135.1, 136.9, 161.8, 166.3, 172.5; ESI-MS obsd 767.3578, calcd 767.3592 [$(M + H)^+$, M = $C_{50}H_{46}N_4O_4$]; λ_{abs} (CH_2Cl_2) 356, 381, 526, 768 nm.

3,13-Bis(ethoxycarbonyl)-2,12-di(naphthalen-1-yl)-5-methoxy-8,8,18,18-tetramethylbacteriochlorin (BC-5). Following an established procedure,[43] a solution of **13** (1.00 g, 2.24 mmol, 18 mM)

in HPLC-grade CH_2Cl_2 (124 mL) was treated first with DTBP (9.9 mL, 45 mmol, 360 mM) and second with TMSOTf (2.0 mL, 11 mmol, 90 mM). The reaction mixture was stirred at room temperature for 16 h. The reaction mixture was quenched by the addition of saturated aqueous $NaHCO_3$. The organic phase was separated, concentrated, and chromatographed (silica, CH_2Cl_2). A single green band was isolated and concentrated to afford a purple/green solid (620 mg, 69%). The ^{1}H NMR spectrum indicated a mixture of atropisomers (~1 : 1 ratio): ^{1}H NMR (500 MHz, $CDCl_3$) δ −1.37 (br s, 2H), −1.05 (br s, 2H), 0.65–0.68 (m, 6H), 1.04–1.07 (m, 6H), 1.58–1.79 (m, 24H), 4.12–4.18 (m, 4H), 4.27 (s, 6H), 4.31–4.37 (m, 12H), 7.28–7.32 (m, 4H), 7.55 (m, 4H), 7.69 (t, J = 8.8 Hz, 2H), 7.77–7.83 (m, 6H), 7.91–7.93 (m, 2H), 8.04–8.08 (m, 6H), 8.15 (d, J = 8.5 Hz, 4H), 8.18 (s, 2H), 8.29 (s, 2H), 9.72 (s, 2H); ^{13}C NMR (100 MHz, $CDCl_3$) δ 13.4, 14.2, 30.8, 30.9, 31.0, 31.1, 45.7, 46.2, 48.2, 51.8, 60.5, 61.7, 64.7, 96.7, 98.3, 98.5, 120.7, 125.2, 125.5, 126.0, 126.2, 126.3, 127.02, 127.04, 127.7, 128.27, 128.31, 128.48, 128.53, 129.2, 130.0, 130.7, 130.8, 131.8, 133.0, 133.4, 133.7, 133.96, 134.01, 134.2, 134.6, 135.3, 135.5, 135.7, 136.5, 157.1, 161.7, 166.3, 168.1, 169.2, 172.9; ESI-MS obsd 797.3689, calcd 797.3697 [$(M + H)^+$, M = $C_{51}H_{48}N_4O_5$]; λ_{abs} (CH_2Cl_2) 371, 528, 748 nm.

In(III)X-3,13-Bis(ethoxycarbonyl)-2,12-di(naphthalen-1-yl)-8,8,18,18-tetramethylbacteriochlorin (BC-6). Following an established procedure,[72] a solution of **BC-4** (25 mg, 0.033 mmol) in anhydrous THF (1.6 mL) was treated with NaH (13 mg, 0.33 mmol, 60% in mineral oil). The reaction mixture was stirred at room temperature for 5 min, whereupon the solution turned from purple/green to bright green. The mixture was then treated with $InBr_3$ (584 mg, 1.65 mmol), affording immediately a bright pink solution. The mixture was then stirred at 50 °C for 16 h. The reaction mixture was quenched by the addition of saturated aqueous $NaHCO_3$. The organic phase was separated, concentrated, and chromatographed [silica, CH_2Cl_2/ethyl acetate (9 : 1)]. The first band (green) was the free-base starting material (10 mg), followed by a pink band (7.5 mg, 25%): ^{1}H NMR (400 MHz, $CDCl_3$) δ 0.63–0.68 (m, 6H), 1.50–1.52 (m, 3H), 1.72–1.79 (m, 6H), 1.87–1.90 (m, 3H), 3.87–4.16 (m, 4H), 4.33–4.42 (m, 2H), 4.51–4.60 (m, 2H), 7.17–7.22 (m, 2H), 7.34–7.39 (m, 1H), 7.42–7.51 (m, 2H), 7.57–7.61 (m, 1H), 7.64–7.67 (m, 1H), 7.73–7.77 (m, 1H), 7.84–7.88 (m, 2H), 7.96–7.98 (m, 1H), 8.04–8.16 (m, 4H), 8.27 (s, 1H), 8.30 (s, 1H), 9.82 (s, 1H); ESI-MS obsd 879.2387, calcd 879.2401 [$(M - X)^+$, M = $C_{50}H_{44}InXN_4O_4$]; λ_{abs} (CH_2Cl_2) 355, 392, 565, 793 nm. The identity of the indium(III) counterion, X, is not known with certainty; the yield is calculated assuming X = Cl.

Zn(II)-3,13-Bis(ethoxycarbonyl)-2,12-di(naphthalen-1-yl)-5-methoxy-8,8,18,18-tetramethylbacteriochlorin (BC-7). Following an established procedure,[72] a mixture of **BC-5** (48 mg, 0.060 mmol) and NaH (43 mg, 1.8 mmol) was added to DMSO (6.0 mL) under argon and stirred for 5 min. $Zn(OAc)_2{\cdot}2H_2O$ (658 mg, 3.0 mmol, 50 eq.) was then added and the suspension was stirred for 16 h in an oil bath at 60 °C. The crude mixture was washed with brine and extracted by ethyl acetate. The combined ethyl acetate extract was dried (Na_2SO_4), concentrated and chromatographed [silica, hexanes/ethyl acetate (3 : 2)] to afford a reddish solid (41 mg, 80%). The ^{1}H NMR spectrum indicated a mixture of atropisomers (~1 : 1 ratio): ^{1}H NMR (500 MHz, $CDCl_3$) δ 0.570.61 (m, 6H), 1.02–1.07 (m, 6H), 1.56–1.79 (m, 24H), 3.97–4.08 (m, 4H), 4.18 (s, 6H), 4.27–4.35 (m, 12H), 7.27–7.31 (m, 4H), 7.49–7.55 (m, 4H), 7.70–7.87 (m, 10H), 7.92–7.99 (m, 2H), 8.03–8.12 (m, 10H), 8.19 (s, 2H), 9.61 (s, 2H); ^{13}C NMR (100 MHz, $CDCl_3$) δ 13.3, 14.1, 30.3, 30.7, 30.8, 44.7, 45.0, 47.2, 50.6, 60.0, 61.4, 64.3, 97.6, 99.3, 123.8, 123.9, 125.2, 125.5, 125.8, 125.9, 126.1, 127.4, 127.9, 128.0, 128.2, 128.3, 128.6, 129.5, 129.7, 130.0, 130.1, 132.9, 133.6, 134.0, 134.6, 135.4, 136.9, 139.7, 140.3, 144.5, 145.7, 146.5, 151.6, 156.2, 164.8, 167.1, 167.8, 169.5; MALDI-MS obsd 859.0533; ESI-MS obsd 858.2753, calcd 858.2754 (M^+, M = $C_{51}H_{46}N_4O_5Zn$); λ_{abs} (CH_2Cl_2) 352, 384, 550, 762 nm.

2,12-Bis(ethoxycarbonyl)-10-methoxy-8,8,18,18-tetramethyl-3,13-di(naphthalen-1-yl)bacteriochlorin (BC-8). Following a literature procedure[45] with slight modification, a solution of **19** (39 mg, 0.087 mmol) in CH_2Cl_2 (4.4 mL) was treated with DTBP (400 μL, 1.78 mmol) followed by TMSOTf (80 μL, 0.44 mmol). The reaction mixture was stirred under a nitrogen atmosphere at room temperature for 15 h, and then diluted with CH_2Cl_2 and washed with saturated aqueous $NaHCO_3$. The organic layer was dried (Na_2SO_4) and filtered. The filtrate was concentrated under reduced pressure. Column chromatography [deactivated silica, hexanes/CH_2Cl_2 (3 : 1 to 2 : 1)] afforded a dark purple solid (16.0 mg, 44%): the ^{1}H NMR spectrum indicated a mixture of atropisomers (~1 : 1 ratio): ^{1}H NMR (600 MHz, $CDCl_3$) δ −1.20 (br s, 2H), −0.88 (br s, 2H), 0.67–0.72 (m, 6H), 1.00–1.05 (m, 6H), 1.87–2.06 (m, 24H), 4.07–4.19 (m, 12H), 4.20–4.23 (m, 6H), 4.25–4.33 (m, 4H), 7.26–7.32 (m, 4H), 7.49–7.55 (m, 4H), 7.58–7.68 (m, 4H), 7.77–7.82 (m, 4H), 7.84–7.89 (m, 2H), 7.98–8.08 (m, 6H), 8.15 (d, J = 7.8 Hz, 4H), 8.21 (s, 2H), 8.27 (s, 2H), 9.60 (s, 2H); ^{13}C NMR (150 MHz, $CDCl_3$) δ 13.23, 13.77, 26.60, 29.22, 29.33, 29.71, 30.14, 30.70, 30.74, 30.90, 30.95, 46.10, 47.30, 53.83, 60.20, 61.32, 68.54, 95.99, 98.68, 100.1, 100.5, 115.2, 120.9, 125.0, 125.2, 125.6, 125.8, 126.0, 126.05, 126.06, 126.10, 126.9, 127.3, 128.03, 128.05, 128.2, 128.8, 129.3, 129.41, 129.44, 130.4, 130.5, 131.84, 131.86, 132.5, 132.78, 132.80, 133.4, 133.6, 133.9, 134.02, 134.05, 134.4, 136.4, 137.1, 137.2, 158.2, 160.0, 162.5, 165.7, 166.7, 167.5, 173.7; ESI-MS obsd 797.3697, calcd 797.3698 [$(M + H)^+$, M = $C_{51}H_{48}N_4O_5$]; λ_{abs} (toluene) 362, 375, 531, 752 nm.

3,13-Dibromo-2,12-bis(ethoxycarbonyl)-8,8,18,18-tetramethylbacteriochlorin (BC-10). Following a literature procedure[45] with modification, TMSOTf (2.71 mL, 15.0 mmol) was added to a solution of **25** (798.6 mg, 2.000 mmol) and DTBP (13.2 mL, 60.0 mmol) in 1,2-dichloroethane (400 mL) at room temperature. The reaction mixture was heated at reflux for 11 h and then allowed to cool to room temperature. The reaction mixture was quenched with pyridine (1.61 mL, 200 mmol) and concentrated under reduced pressure. Column chromatography [deactivated silica, hexanes/CH_2Cl_2/MeCN (500 : 50 : 1 to 100 : 10 : 1)] afforded the title compound as a dark purple solid (196.5 mg, 29% and the 10-methoxy derivative thereof, namely 3,13-dibromo-2,12-bis(ethoxycarbonyl)-10-methoxy-8,8,18,18-tetramethylbacteriochlorin (**BC-11**)) as a dark purple solid (250.2 mg, 36%). Data for the title compound: ^{1}H NMR (400 MHz, $CDCl_3$) δ 1.77 (t, J = 7.2 Hz, 6H), 1.94 (s, 12H), 4.38 (s, 4H), 4.82 (q, J = 7.2 Hz, 4H), 8.95 (s, 2H), 9.56 (s, 2H);

^{13}C NMR (100 MHz, $CDCl_3$) δ 14.8, 31.0, 46.4, 51.4, 61.6, 97.7, 99.1, 115.6, 121.2, 132.4, 135.7, 161.1, 164.7, 173.8; ESI-MS obsd 671.0858, calcd 671.0863 [$(M + H)^+$, M = $C_{30}H_{32}Br_2N_4O_4$]; λ_{abs} (toluene) 357, 385, 528, 731, 772 nm.

Data for **BC-11**: ^{1}H NMR (400 MHz, $CDCl_3$) δ 1.58 (t, J = 7.0 Hz, 3H), 1.74 (t, J = 7.0 Hz, 3H), 1.91 (s, 6H), 2.02 (s, 6H), 4.15 (s, 3H), 4.31 (s, 2H), 4.34 (s, 2H), 4.76 (q, J = 7.0 Hz, 2H), 4.80 (q, J = 7.0 Hz, 2H), 8.72 (s, 1H), 8.87 (s, 1H) 9.41 (s, 1H); ^{13}C NMR (100 MHz, $CDCl_3$) δ 14.5, 14.8, 29.3, 30.9, 46.4, 47.4, 51.1, 54.0, 61.6, 62.4, 68.8, 96.5, 98.1, 99.5, 109.9, 116.2, 120.8, 125.7, 129.6, 131.3, 132.0, 136.3, 137.0, 159.1, 160.7, 164.6, 166.8, 167.1, 174.1; ESI-MS obsd 701.0974, calcd 701.0969 [$(M + H)^+$, M = $C_{31}H_{34}Br_2N_4O_5$]; λ_{abs} (toluene) 360, 372, 532, 719, 756 nm.

3,13-Bis(8-bromonaphthalen-1-yl)-2,12-bis(ethoxycarbonyl)-8,8,18,18-tetramethylbacteriochlorin (BC-12). A suspension of **BC-10** (6.7 mg, 0.010 mmol), (8-bromonaphthalen-1-yl)boronic acid (25.1 mg, 0.100 mmol), K_2CO_3 (27.6 mg, 0.200 mmol), and $Pd(PPh_3)_4$ (1.2 mg, 0.0010 mmol) in toluene (333 μL) and DMF (167 μL) was deaerated by two freeze–pump–thaw cycles. The resulting mixture was heated to 100 °C for 14 h and then allowed to cool to room temperature. The mixture was passed through a basic alumina pad (CH_2Cl_2 as an eluent). The eluent was concentrated under reduced pressure. Column chromatography [deactivated silica, hexanes/CH_2Cl_2 (9 : 2)] afforded a dark purple solid (4.5 mg, 49%). ^{1}H and ^{13}C NMR spectra indicated a mixture of atropisomers (~1 : 1 ratio). Two distinguishable spots were found on TLC analysis with close R_f values [0.23 and 0.26, deactivated silica, 3 × hexanes/ethyl acetate (9 : 1)]. This sample was used as a mixture of atropisomers in the next step. Data for the title compound: ^{1}H NMR (400 MHz, $CDCl_3$) δ −1.0 (s, 4H), 0.72 (t, J = 7.2 Hz, 12H), 1.90 (s, 6H), 1.91 (s, 6H), 1.95 (s, 6H), 1.96 (s, 6H), 4.32–4.06 (m, 16H), 7.38 (t, J = 7.8 Hz, 4H), 7.84–7.66 (m, 12H), 8.08 (d, J = 8.4 Hz, 4H), 8.16 (d, J = 8.4 Hz, 4H), 8.28 (s, 4H), 9.76 (s, 4H); ^{13}C NMR (100 MHz, $CDCl_3$) δ 13.4, 30.9, 31.6, 31.2, 31.3, 46.4, 51.4, 60.2, 97.4, 100.2, 121.2, 121.3, 122.0, 125.1, 126.2, 129.3, 129.9, 132.0, 132.8, 132.9, 133.6, 133.8, 134.9, 135.80, 135.83, 135.9, 139.34, 139.36, 160.3, 165.9, 173.4; ESI-MS obsd 922.1715, calcd 922.1724 [$(M)^+$, M = $C_{50}H_{44}Br_2N_4O_4$].

Phen-BC. A suspension of **BC-12** (8.6 mg, 0.0093 mmol), K_2CO_3 (12.9 mg, 0.0933 mmol), 2-dicyclohexylphosphino-2′,6′-dimethoxybiphenyl (11.5 mg, 0.0280 mmol), and $Pd(OAc)_2$ (2.1 mg, 0.0094 mmol) in DMF (1.00 mL) was deaerated by two freeze–pump–thaw cycles. The resulting mixture was heated to 80 °C for 5.5 h, 100 °C for 0.5 h, and then allowed to cool to room temperature. The mixture was diluted with CH_2Cl_2 and passed through deactivated silica. The eluent was concentrated under reduced pressure. Column chromatography [deactivated silica, hexanes/CH_2Cl_2 (11 : 9)] afforded a dark green solid (2.6 mg, 37%): ^{1}H NMR (300 MHz, $CDCl_3$) δ 1.57 (s, 12H), 1.72 (t, J = 7.0 Hz, 6H), 1.97 (s, 2H), 4.31 (s, 4H), 4.88 (q, J = 7.0 Hz, 4H), 7.58–7.80 (m, 4H), 7.76–8.02 (m, 4H), 8.30–8.48 (m, 2H), 8.35 (s, 2H), 8.84–9.06 (m, 2H); ^{13}C NMR (125 MHz, $CDCl_3$) δ 14.8, 29.3, 46.1, 55.9, 61.7, 97.5, 110.1, 115.1, 126.4, 126.7, 126.8, 127.4, 127.5, 128.2, 128.3, 129.8, 133.5, 133.6, 134.0, 135.9, 161.6, 166.8, 168.2; ESI-MS obsd 762.3191, calcd 762.3201 [$(M)^+$, M = $C_{50}H_{42}N_4O_4$]; λ_{abs} (toluene) 306, 336, 383, 425, 622, 675, 829, 913 nm.

3,13-Bis(2-bromophenyl)-2,12-bis(ethoxycarbonyl)-8,8,18,18-tetramethylbacteriochlorin (BC-13). A suspension of **BC-10** (6.7 mg, 0.010 mmol), (2-bromophenyl)boronic acid (20.1 mg, 0.100 mmol), K_2CO_3 (27.6 mg, 0.200 mmol), and $Pd(PPh_3)_4$ (3.5 mg, 0.0030 mmol) in toluene (333 μL) and DMF (167 μL) was deaerated by two freeze–pump–thaw cycles. The resulting mixture was heated to 100 °C for 5 h and then allowed to cool to room temperature. The mixture was passed through a pad of basic alumina (CH_2Cl_2 as an eluent). The eluent was concentrated under reduced pressure. Column chromatography [deactivated silica, hexanes/CH_2Cl_2 (9 : 1 to 8 : 1)] afforded a dark purple solid (7.0 mg, 85%). ^{1}H and ^{13}C NMR spectra indicated a mixture of atropisomers (~1 : 1 ratio). Two distinguishable spots were found on TLC analysis with close R_f values [0.33 and 0.37, deactivated silica, 3 × hexanes/ethyl acetate (9 : 1)]. This sample was used as a mixture of atropisomers in the next step. Data for the title compound: ^{1}H NMR (400 MHz, $CDCl_3$) δ −1.14 (s, 4H), 1.24 (t, J = 7.2 Hz, 12H), 1.94 (s, 12H), 1.96 (s, 6H), 1.97 (s, 6H), 4.27 (s, 8H), 4.44 (dq, J = 7.2, 10.7 Hz, 4H), 4.53 (dq, J = 7.2, 10.7 Hz, 4H), 7.47–7.58 (m, 4H), 7.58–7.69 (m, 4H), 7.69–7.83 (m, 4H), 7.87–7.98 (m, 4H), 9.73 (s, 4H), 8.29 (s, 4H); ^{13}C NMR (100 MHz, $CDCl_3$) δ 14.0, 31.0, 31.1, 31.2, 31.3, 46.4, 51.4, 60.8, 97.7, 99.3, 120.57, 120.58, 125.91, 125.94, 126.80, 126.83, 129.6, 132.4, 132.5, 132.9, 133.0, 133.1, 135.6, 137.4, 137.5, 137.6, 160.6, 165.7, 173.6; ESI-MS obsd 822.1400, calcd 822.1411 [$(M)^+$, M = $C_{42}H_{40}Br_2N_4O_4$].

Benz-BC. A suspension of **BC-13** (52.0 mg, 0.0631 mmol), K_2CO_3 (43.6 mg, 0.315 mmol), tricyclohexylphosphine tetrafluoroborate (69.7 mg, 0.189 mmol), and $Pd(OAc)_2$ (14.2 mg, 0.0632 mmol) in DMF (6.3 mL) was deaerated by three freeze–pump–thaw cycles. The resulting mixture was heated to 110 °C for 2 h and then allowed to cool to room temperature. The mixture was diluted with CH_2Cl_2 (40 mL) and washed with H_2O (50 mL) and brine (20 mL). The organic layer was dried (Na_2SO_4) and passed through deactivated silica. The eluent was concentrated under reduced pressure. The residue was washed with MeOH, MeCN, and hexanes to give a dark green solid (33.3 mg, 80%): ^{1}H NMR (400 MHz, $CDCl_3$) δ 1.69 (t, J = 7.2 Hz, 6H), 1.78 (s, 12H), 2.89 (s, 2H), 4.00 (s, 4H), 4.71 (q, J = 7.2, 4H), 6.97–7.04 (m, 2H), 7.04–7.10 (m, 2H), 7.49–7.54 (m, 2H), 8.02–8.06 (m, 2H), 8.71 (s, 2H); ^{13}C NMR (175 MHz, $CDCl_3$) δ 14.9, 30.7, 46.5, 49.1, 61.1, 101.0, 113.1, 113.4, 123.6, 126.5, 127.4, 129.3, 136.5, 141.3, 142.1, 143.9, 149.1, 159.0, 165.3, 174.7; ESI-MS obsd 662.2881, calcd 662.2899 [$(M)^+$, M = $C_{42}H_{38}N_4O_4$]; λ_{abs} (toluene) 311, 403, 425, 442, 488, 658, 719, 821, 914, 1033 nm.

Photophysical measurements

Photophysical studies were carried out on samples in dilute (μM) argon-purged solutions of toluene. Excitation and detection bandwidths of 5 nm were employed for fluorescence spectra. Fluorescence quantum yields were determined for argon-purged samples relative to standards *meso*-tetraphenylporphyrin (Φ_f = 0.070 in toluene with ambient O_2),[98] **H-BC** (Φ_f = 0.14 in argon-purged

toluene)[85] and the zinc chelate of **I2-BC** (Φ_f = 0.031 in argon-purged toluene).[5] Each emission spectrum was integrated to include both the origin and vibronic satellite features. For each Φ_f determination, the emission spectrum was acquired using at least three excitation wavelengths spanning the Soret and Q_x (and in some cases Q_y) regions with good agreement, and the results were averaged. S_1 lifetimes were determined by time-correlated single photon counting (TCSPC) fluorescence spectroscopy and by transient absorption (TA) spectroscopy, both employing ~100 fs excitation flashes from an ultrafast laser system.[73]

Molar absorption coefficients

The molar absorption coefficients were determined by dissolving a known quantity of each bacteriochlorin (1.01–2.66 mg) in toluene (5.00 mL). Then a known amount (40.0–100.0 μL) of this solution was diluted to 5.00 mL with toluene. The absorption spectrum was recorded at room temperature. The averages of 5 runs were calculated: **BC-10** (ε_{756nm} = 36 800 M^{-1} cm^{-1}, ε_{772nm} = 135 000 M^{-1} cm^{-1}); **BC-11** (ε_{756nm} = 117 000 M^{-1} cm^{-1}, ε_{772nm} = 20 800 M^{-1} cm^{-1}).

Density functional theory calculations

DFT calculations were performed with Gaussian 09 version D.01.[99] Calculations used the polarization continuum model for the arrays in toluene. Molecular geometries were fully optimized using the hybrid B3LYP functional and the basis set 6-31G*. These calculations used Gaussian defaults with the exception of keyword Int = (Grid = Ultrafine, Acc2E = 14). TDDFT calculations used the long-range corrected ωB97XD functional and the basis set 6-31++G**. These calculations used Gaussian defaults with the exception of keywords TD (nStates = 16), Int = (Grid = Ultrafine, Acc2E = 14), and Pop = Full.

Conflicts of interest

The authors declare no competing financial interests.

Acknowledgements

This work was supported by a grant from the Chemical Sciences, Geosciences and Biosciences Division, Office of Basic Energy Sciences, of the U. S. Department of Energy (DE-FG02-05ER15661).

References

1 C. Brückner, L. Samankumara and J. Ogikubo, in *Handbook of Porphyrin Science*, ed. K. M. Kadish, K. M. Smith and R. Guilard, World Scientific Publishing Co. Pte. Ltd, Singapore, 2012, vol. 17, pp. 1–112.
2 H. Scheer, in *Chlorophylls and Bacteriochlorophylls. Biochemistry, Biophysics, Functions and Applications*, ed. B. Grimm, R. J. Porra, W. Rüdiger and H. Scheer, Springer, Dordrecht, The Netherlands, 2006, pp. 1–26.
3 M. A. Grin, A. F. Mironov and A. A. Shtil, *Anti-Cancer Agents Med. Chem.*, 2008, **8**, 683–697.
4 M. A. Grin and A. F. Mironov, *Russ. Chem. Bull., Int. Ed.*, 2016, **65**, 333–349.
5 P. Vairaprakash, E. Yang, T. Sahin, M. Taniguchi, M. Krayer, J. R. Diers, A. Wang, D. M. Niedzwiedzki, C. Kirmaier, J. S. Lindsey, D. F. Bocian and D. Holten, *J. Phys. Chem. B*, 2015, **119**, 4382–4395.
6 M. Krayer, E. Yang, J. R. Diers, D. F. Bocian, D. Holten and J. S. Lindsey, *New J. Chem.*, 2011, **35**, 587–601.
7 T. D. Lash, in *The Porphyrin Handbook*, ed. K. M. Kadish, K. M. Smith and R. Guilard, Academic Press, San Diego, 2000, vol. 2, pp. 125–199.
8 T. D. Lash, *J. Porphyrins Phthalocyanines*, 2001, **5**, 267–288.
9 S. Fox and R. W. Boyle, *Tetrahedron*, 2006, **62**, 10039–10054.
10 J. P. Lewtak and D. T. Gryko, *Chem. Commun.*, 2012, **48**, 10069–10086.
11 A. M. V. M. Pereira, S. Richeter, C. Jeandon, J.-P. Gisselbrecht, J. Wytko and R. Ruppert, *J. Porphyrins Phthalocyanines*, 2012, **16**, 464–478.
12 H. Mori, T. Tanaka and A. Osuka, *J. Mater. Chem. C*, 2013, **1**, 2500–2519.
13 O. Yamane, K.-I. Sugiura, H. Miyasaka, K. Nakamura, T. Fujimoto, K. Nakamura, T. Kaneda, Y. Sakata and M. Yamashita, *Chem. Lett.*, 2004, **33**, 40–41.
14 K. Kurotobi, K. S. Kim, S. B. Noh, D. Kim and A. Osuka, *Angew. Chem., Int. Ed.*, 2006, **45**, 3944–3947.
15 M. Tanaka, S. Hayashi, S. Eu, T. Umeyama, Y. Matano and H. Imahori, *Chem. Commun.*, 2007, 2069–2071.
16 N. K. S. Davis, A. L. Thompson and H. L. Anderson, *Org. Lett.*, 2010, **12**, 2124–2127.
17 C. Jiao, K.-W. Huang, C. Chi and J. Wu, *J. Org. Chem.*, 2011, **76**, 661–664.
18 N. K. S. Davis, A. L. Thompson and H. L. Anderson, *J. Am. Chem. Soc.*, 2011, **133**, 30–31.
19 L. Jiang, J. T. Engle, L. Sirk, C. S. Hartley, C. J. Ziegler and H. Wang, *Org. Lett.*, 2011, **13**, 3020–3023.
20 J. P. Lewtak, D. Gryko, D. Bao, E. Sebai, O. Vakuliuk, M. Ścigaj and D. T. Gryko, *Org. Biomol. Chem.*, 2011, **9**, 8178–8181.
21 V. V. Diev, C. W. Schlenker, K. Hanson, Q. Zhong, J. D. Zimmerman, S. R. Forrest and M. E. Thompson, *J. Org. Chem.*, 2012, **77**, 143–159.
22 N. Fukui, W. Y. Cha, S. Lee, S. Tokuji, D. Kim, H. Yorimitsu and A. Osuka, *Angew. Chem., Int. Ed.*, 2013, **52**, 9728–9732.
23 P. Chen, Y. Fang, K. M. Kadish, J. P. Lewtak, D. Koszelewski, A. Janiga and D. T. Gryko, *Inorg. Chem.*, 2013, **52**, 9532–9538.
24 K. Ota, T. Tanaka and A. Osuka, *Org. Lett.*, 2014, **16**, 2974–2977.
25 J. Luo, S. Lee, M. Son, B. Zheng, K.-W. Huang, Q. Qi, W. Zeng, G. Li, D. Kim and J. Wu, *Chem. – Eur. J.*, 2015, **21**, 3708–3715.
26 N. Fukui, W. Cha, D. Shimizu, J. Oh, K. Furukawa, H. Yorimitsu, D. Kim and A. Osuka, *Chem. Sci.*, 2016, **8**, 189–199.
27 S. Fox and R. W. Boyle, *Chem. Commun.*, 2004, 1322–1323.

28 A. N. Cammidge, P. J. Scaife, G. Berber and D. L. Hughes, *Org. Lett.*, 2005, **7**, 3413–3416.
29 M. Pawlicki, M. Morisue, N. K. S. Davis, D. G. McLean, J. E. Haley, E. Beuerman, M. Drobizhev, A. Rebane, A. L. Thompson, S. I. Pascu, G. Accorsi, N. Armaroli and H. L. Anderson, *Chem. Sci.*, 2012, **3**, 1541–1547.
30 T. Ishizuka, Y. Saegusa, Y. Shiota, K. Ohtake, K. Yoshizawa and T. Kojima, *Chem. Commun.*, 2013, **49**, 5939–5941.
31 Y. Saegusa, T. Ishizuka, K. Komamura, S. Shimizu, H. Kotani, N. Kobayashi and T. Kojima, *Phys. Chem. Chem. Phys.*, 2015, **17**, 15001–15011.
32 N. Ono, H. Yamada and T. Okujima, in *Handbook of Porphyrin Science*, ed. K. M. Kadish, K. M. Smith and R. Guilard, World Scientific Publishing Co. Pte. Ltd, Singapore, 2010, vol. 2, pp. 1–102.
33 A. V. Cheprakov, in *Handbook of Porphyrin Science*, ed. K. M. Kadish, K. M. Smith and R. Guilard, World Scientific Publishing Co. Pte. Ltd, Singapore, 2011, vol. 13, pp. 1–149.
34 S. V. Dudkin, E. A. Makarova and E. A. Lukyanets, *Russ. Chem. Rev.*, 2016, **85**, 700–730.
35 M. M. Pereira, C. J. P. Monteiro, A. V. C. Simões, S. M. A. Pinto, A. R. Abreu, G. F. F. Sá, E. F. F. Silva, L. B. Rocha, J. M. Dbrowski, S. J. Formosinho, S. Simões and L. G. Arnaut, *Tetrahedron*, 2010, **66**, 9545–9551.
36 M. M. Pereira, A. R. Abreu, N. P. F. Goncalves, M. J. F. Calvete, A. V. C. Simões, C. J. P. Monteiro, L. G. Arnaut, M. E. Eusébio and J. Canotilho, *Green Chem.*, 2012, **14**, 1666–1672.
37 M. Taniguchi and J. S. Lindsey, *Chem. Rev.*, 2017, **117**, 344–535.
38 C. Brückner, *Acc. Chem. Res.*, 2016, **49**, 1080–1092.
39 Y. Chen, G. Li and R. K. Pandey, *Curr. Org. Chem.*, 2004, **8**, 1105–1134.
40 T. G. Minehan and Y. Kishi, *Angew. Chem., Int. Ed.*, 1999, **38**, 923–925.
41 W. Wang and Y. Kishi, *Org. Lett.*, 1999, **1**, 1129–1132.
42 H.-J. Kim and J. S. Lindsey, *J. Org. Chem.*, 2005, **70**, 5475–5486.
43 M. Krayer, M. Ptaszek, H. J. Kim, K. R. Meneely, D. Fan, K. Secor and J. S. Lindsey, *J. Org. Chem.*, 2010, **75**, 1016–1039.
44 S. Zhang, H.-J. Kim, Q. Tang, E. Yang, D. F. Bocian, D. Holten and J. S. Lindsey, *New J. Chem.*, 2016, **40**, 5942–5956.
45 Y. Liu and J. S. Lindsey, *J. Org. Chem.*, 2016, **81**, 11882–11897.
46 S. Zhang and J. S. Lindsey, *J. Org. Chem.*, 2017, **82**, 2489–2504.
47 M. N. Reddy, S. Zhang, H.-J. Kim, O. Mass, M. Taniguchi and J. S. Lindsey, *Molecules*, 2017, **22**, 634.
48 Z. Yu and M. Ptaszek, *J. Org. Chem.*, 2013, **78**, 10678–10691.
49 Z. Yu, C. Pancholi, G. V. Bhagavathy, H. S. Kang, J. K. Nguyen and M. Ptaszek, *J. Org. Chem.*, 2014, **79**, 7910–7925.
50 N. N. Esemoto, Z. Yu, L. Wiratan, A. Satraitis and M. Ptaszek, *Org. Lett.*, 2016, **18**, 4590–4593.
51 A. Meares, A. Satraitis, J. Akhigbe, N. Santhanam, S. Swaminathan, M. Ehudin and M. Ptaszek, *J. Org. Chem.*, 2017, **82**, 6054–6070.
52 A. Meares, A. Satraitis and M. Ptaszek, *J. Org. Chem.*, 2017, **82**, 13068–13075.
53 N. N. Esemoto, A. Satraitis, L. Wiratan and M. Ptaszek, *Inorg. Chem.*, 2018, **57**, 2977–2988.
54 F. F. de Assis, M. A. B. Ferreira, T. J. Brocksom and K. T. de Oliveira, *Org. Biomol. Chem.*, 2016, **14**, 1402–1412.
55 S. Chakraborty, H.-C. You, C.-K. Huang, B.-Z. Lin, C.-L. Wang, M.-C. Tsai, C.-L. Liu and C.-Y. Lin, *J. Phys. Chem. C*, 2017, **121**, 7081–7087.
56 M. P. Balany and D. H. Kim, *J. Phys. Chem. A*, 2017, **121**, 6660–6669.
57 F. Ponsot, N. Desbois, L. Bucher, M. Berthelot, P. Mondal, C. P. Gros and A. Romieu, *Dyes Pigm.*, 2019, **160**, 747–756.
58 A. Boudif, S. Gimenez, B. Loock and M. Momenteau, *Can. J. Chem.*, 1998, **76**, 1215–1219.
59 R. Deshpande, L. Jiang, G. Schmidt, J. Rakovan, X. Wang, K. Wheeler and H. Wang, *Org. Lett.*, 2009, **11**, 4251–4253.
60 G. Pomarico, S. Nardis, R. Paolesse, O. C. Ongayi, B. H. Courtney, F. R. Fronczek and M. G. H. Vicente, *J. Org. Chem.*, 2011, **76**, 3765–3773.
61 R. Deshpande, B. Wang, L. Dai, L. Jiang, C. S. Hartley, S. Zou, H. Wang and L. Kerr, *Chem. – Asian J.*, 2012, **7**, 2662–2669.
62 G. Pomarico, S. Nardis, M. Stefanelli, D. O. Cicero, M. G. H. Vicente, Y. Fang, P. Chen, K. M. Kadish and R. Paolesse, *Inorg. Chem.*, 2013, **52**, 8834–8844.
63 L. Jiang, J. T. Engle, R. A. Zaenglein, A. Matus, C. J. Ziegler, H. Wang and M. J. Stillman, *Chem. – Eur. J.*, 2014, **20**, 13865–13870.
64 R. G. W. Jinadasa, Y. Fang, S. Kumar, A. J. Osinski, X. Jiang, C. J. Ziegler, K. M. Kadish and H. Wang, *J. Org. Chem.*, 2015, **80**, 12076–12087.
65 R. G. W. Jinadasa, Y. Fang, Y. Deng, R. Deshpande, X. Jiang, K. M. Kadish and H. Wang, *RSC Adv.*, 2015, **5**, 51489–51492.
66 Y. Hu, M. B. Thomas, R. G. W. Jinadasa, H. Wang and F. D'Souza, *Chem. – Eur. J.*, 2017, **23**, 12805–12814.
67 R. G. W. Jinadasa, M. B. Thomas, Y. Hu, F. D'Souza and H. Wang, *Phys. Chem. Chem. Phys.*, 2017, **19**, 13182–13188.
68 B. H. Novak and T. D. Lash, *J. Org. Chem.*, 1998, **63**, 3998–4010.
69 T. D. Lash and B. H. Novak, *Angew. Chem., Int. Ed. Engl.*, 1995, **34**, 683–685.
70 J. H. Chang and H. Shin, *Org. Process Res. Dev.*, 2008, **12**, 291–293.
71 O. Mass and J. S. Lindsey, *J. Org. Chem.*, 2011, **76**, 9478–9487.
72 C.-Y. Chen, E. Sun, D. Fan, M. Taniguchi, B. E. McDowell, E. Yang, J. R. Diers, D. F. Bocian, D. Holten and J. S. Lindsey, *Inorg. Chem.*, 2012, **51**, 9443–9464.
73 Z. Wu, H. Fujita, N. C. M. Magdaong, J. R. Diers, D. Hood, S. Allu, D. M. Niedzwiedzki, C. Kirmaier, D. F. Bocian, D. Holten and J. S. Lindsey, *New J. Chem.*, 2019, DOI: 10.1039/c9nj01114e.
74 N. De Kimpe, in *Encyclopedia of Reagents for Organic Synthesis*, ed. L. Paquette, John Wiley & Sons, 2009, vol. 11, pp. 9100–9102.
75 L. Yu, K. Muthukumaran, I. V. Sazanovich, C. Kirmaier, E. Hindin, J. R. Diers, P. D. Boyle, D. F. Bocian, D. Holten and J. S. Lindsey, *Inorg. Chem.*, 2003, **42**, 6629–6647.
76 H.-J. Kim, D. K. Dogutan, M. Ptaszek and J. S. Lindsey, *Tetrahedron*, 2007, **63**, 37–55.

77 M. Krayer, T. Balasubramanian, C. Ruzié, M. Ptaszek, D. L. Cramer, M. Taniguchi and J. S. Lindsey, *J. Porphyrins Phthalocyanines*, 2009, **13**, 1098–1110.
78 M. Liu, M. Ptaszek, O. Mass, D. F. Minkler, R. D. Sommer, J. Bhaumik and J. S. Lindsey, *New J. Chem.*, 2014, **38**, 1717–1730.
79 S. Zhang, M. N. Reddy, O. Mass, H.-J. Kim, G. Hu and J. S. Lindsey, *New J. Chem.*, 2017, **41**, 11170–11189.
80 F. Camps, J. Coll and A. Parente, *Synthesis*, 1978, 215–216.
81 W. G. O'Neal, W. P. Roberts, I. Ghosh, H. Wang and P. A. Jacobi, *J. Org. Chem.*, 2006, **71**, 3472–3480.
82 A. Bahl, W. Grahn, S. Stadler, F. Feiner, G. Bourhill, C. Bräuchle, A. Reisner and P. G. Jones, *Angew. Chem., Int. Ed. Engl.*, 1995, **34**, 1485–1488.
83 A. Bahl, W. Grahn and P. G. Jones, *Acta Crystallogr., Sect. C: Cryst. Struct. Commun.*, 1996, **52**, 2014–2017.
84 Y. Liu, S. Allu, M. N. Reddy, D. Hood, J. R. Diers, D. F. Bocian, D. Holten and J. S. Lindsey, *New J. Chem.*, 2017, **41**, 4360–4376.
85 E. Yang, C. Kirmaier, M. Krayer, M. Taniguchi, H.-J. Kim, J. R. Diers, D. F. Bocian, J. S. Lindsey and D. Holten, *J. Phys. Chem. B*, 2011, **115**, 10801–10816.
86 E. Yang, C. Ruzié, M. Krayer, J. R. Diers, D. M. Niedzwiedzki, C. Kirmaier, J. S. Lindsey, D. F. Bocian and D. Holten, *Photochem. Photobiol.*, 2013, **89**, 586–604.
87 M. Gouterman, *J. Chem. Phys.*, 1959, **30**, 1139–1161.
88 M. Gouterman, *J. Mol. Spectrosc.*, 1961, **6**, 138–163.
89 M. Gouterman, in *The Porphyrins*, ed. D. Dolphin, Academic Press, New York, 1978, vol. 3, pp. 1–165.
90 R. L. Martin, *J. Chem. Phys.*, 2003, **118**, 4775–4777.
91 L. Jean-Gérard, W. Vasseur, F. Scherninski and B. Andrioletti, *Chem. Commun.*, 2018, **54**, 12914–12929.
92 S. He, J. Song, J. Qu and Z. Cheng, *Chem. Soc. Rev.*, 2018, **47**, 4258–4278.
93 F. Ding, Y. Zhan, X. Lu and Y. Sun, *Chem. Sci.*, 2018, **9**, 4370–4380.
94 J. Yuen, J. R. Diers, E. J. Alexy, A. Roy, A. K. Mandal, H. S. Kang, D. M. Niedzwiedzki, C. Kirmaier, J. S. Lindsey, D. F. Bocian and D. Holten, *J. Phys. Chem. A*, 2018, **122**, 7181–7201.
95 T. Jin, *ECS J. Solid State Sci. Technol.*, 2019, **8**, R9–R13.
96 C. J. Reinhardt and J. Chan, *Biochemistry*, 2018, **57**, 194–199.
97 H. S. Jung, P. Verwilst, A. Sharma, J. Shin, J. L. Sessler and J. S. Kim, *Chem. Soc. Rev.*, 2018, **47**, 2280–2297.
98 J. W. Springer, K. M. Faries, J. R. Diers, C. Muthiah, O. Mass, H. L. Kee, C. Kirmaier, J. S. Lindsey, D. F. Bocian and D. Holten, *Photochem. Photobiol.*, 2012, **88**, 651–674.
99 M. J. Frisch, G. W. Trucks, H. B. Schlegel, G. E. Scuseria, M. A. Robb, J. R. Cheeseman, G. Scalmani, V. Barone, B. Mennucci, G. A. Petersson, H. Nakatsuji, M. Caricato, X. Li, H. P. Hratchian, A. F. Izmaylov, J. Bloino, G. Zheng, J. L. Sonnenberg, M. Hada, M. Ehara, K. Toyota, R. Fukuda, J. Hasegawa, M. Ishida, T. Nakajima, Y. Honda, O. Kitao, H. Nakai, T. Vreven, J. A. Montgomery Jr., J. E. Peralta, F. Ogliaro, M. Bearpark, J. J. Heyd, E. Brothers, K. N. Kudin, V. N. Staroverov, R. Kobayashi, J. Normand, K. Raghavachari, A. Rendell, J. C. Burant, S. S. Iyengar, J. Tomasi, M. Cossi, N. Rega, J. M. Millam, M. Klene, J. E. Knox, J. B. Cross, V. Bakken, C. Adamo, J. Jaramillo, R. Gomperts, R. E. Stratmann, O. Yazyev, A. J. Austin, R. Cammi, C. Pomelli, J. W. Ochterski, R. L. Martin, K. Morokuma, V. G. Zakrzewski, G. A. Voth, P. Salvador, J. J. Dannenberg, S. Dapprich, A. D. Daniels, Ö. Farkas, J. B. Foresman, J. V. Ortiz, J. Cioslowski and D. J. Fox, *Gaussian 09, version D.01*, Gaussian, Inc., Wallingford CT, 2009.

